

**NANOTOXICOLOGY:**  
**An Emerging Discipline Evolving from Studies of Ultrafine Particles**  
**Supplemental Web Sections**

**Günter Oberdörster<sup>1</sup>, Eva Oberdörster<sup>2</sup>, Jan Oberdörster<sup>3</sup>**

<sup>1</sup>University of Rochester  
Department of Environmental Medicine  
Rochester, NY

<sup>2</sup>Southern Methodist University  
Department of Biology  
Dallas, TX

<sup>3</sup>Bayer CropScience  
Toxicology Department  
Research Triangle Park, NC

*Corresponding Author:*

Dr. Günter Oberdörster  
University of Rochester  
Department of Environmental Medicine  
575 Elmwood Avenue, MRBx Bldg., Box 850  
Rochester, NY 14642 USA

e-mail: [Gunter.Oberdorster@urmc.rochester.edu](mailto:Gunter.Oberdorster@urmc.rochester.edu)

fax: 585-256-2631; tele: 585-275-3804

## Outline of Nanotoxicology manuscript - WEB SECTIONS

1. Introduction
  - 1.1 Naturally-Occurring and Anthropogenic Nano-Sized Materials
  - 1.2 Physico-Chemical Characteristics as Determinants of Biological Activity
  - 1.3 Human Exposure to Nano-Sized Materials
  - 1.4 Manufactured Nanomaterials in the Environment
2. Review of Toxicology of Airborne Ultrafine Particles
3. Concepts of Nanotoxicology
  - 3.1 Laboratory Rodent Studies
  - 3.2 Ecotoxicological Studies
  - 3.3 ROS Mechanisms of Nano-Sized Particle Toxicity
  - 3.4 Exposure-Dose-Response Considerations
4. Portals of Entry and Target Tissues
  - 4.1 Respiratory Tract
    - 4.1.1 Efficient Deposition of Inhaled Nano-Sized Particles
    - 4.1.2 Disposition of NSP in the Respiratory Tract
      - Classical Clearance Pathways
      - Epithelial Translocation
      - Translocation to the Circulatory System
      - Neuronal Uptake and Translocation
  - 4.2 GI Tract and Skin
5. Risk Assessment
6. Summary and Outlook
7. References
8. Figure Legends
9. Tables

## SUPPLEMENTAL INFORMATION – WEB SECTIONS

### ***1. Introduction***

#### 1.1 Naturally-Occurring and Anthropogenic Nano-Sized Materials

#### 1.2 Physico-Chemical Characteristics as Determinants of Biological Activity

#### 1.3 Human Exposure to Nano-Sized Materials

A few examples of NSP at the workplace and in the environment in the context of an exposure–dose–response paradigm are summarized in Table S-1. Some obvious and not so obvious sources for UFP include tailpipe emissions that, after dilution in highways can reach very high number concentrations of up to ten million particles per cm<sup>3</sup> (Kittelson et al. 2001), UFP in ice rinks from the exhaust of resurfacing machines, even from natural gas-powered equipment (Rundell 2003); generation of UFP during waxing of skis with the potential to result in acute lung injury (Bracco and Favre 1998; Dahlquist et al. 1992); welding fumes (Zimmer et al. 2002); and emissions of power plants, whether fired by coal, oil, or natural gas (Chang et al. in press). Some of many other sources are listed in Table 1, indicating that indeed UFP are ubiquitous in indoor and outdoor air. Indeed, a source emission inventory for the South Coast Air Basin surrounding Los Angeles (USA) estimated a primary UFP emission rate of 13 tons per day (Cass et al. 2000). However, due to heterogeneous and homogeneous coagulation, UFP numbers decrease at higher concentrations rapidly by factors of 10 and more; for example, with increasing distances from highways (Zhu et al. 2002), or with increasing aging times of aerosols.

However, since heterogeneous coagulation of UFP onto accumulation mode particles is a more efficient mechanism for removal of UFP than homogeneous accumulation of same sized particles, therefore the presence of particles in the accumulation mode becomes important. Cleaning up the air by reducing the number of larger accumulation mode particles significantly may cause a longer persistence and thereby increase of the ultrafine mode since the sink for their effective elimination is no longer present. This mechanism is thought to be responsible for an increase in UFP in ambient air of Erfurt, Germany, after the air in that part of the country was cleaned after

the reunification of Germany in order to comply with a lower mass standard for particulate matter in ambient air (Tuch et al. 1997). Specific considerations with regard to the exposure-dose-response paradigm for NP are summarized in Table S-2

#### 1.4 Manufactured Nanomaterials in the Environment

It is estimated that thousands of tons of engineered nanomaterials, primarily fullerenes (at least 1500 tonnes per year) and single-walled and multi-walled nanotubes (SWNT, MWNT; at least 120 tonnes per year), will be produced annually by 2007 (NNI 2004). The uses of these nanomaterials are in a wide range of products, including in fuel and solar cells (fullerenes), as stabilizers in tires (MWNT), in personal care products, and in some plastic products (sunglasses, tennis balls, car-body parts) to name just a few. When considering the nanomaterial life-cycle, one would expect some human exposures during manufacture, use, and disposal of the nanomaterial. In each of these steps, environmental contamination is likely. For example, MWNT are used in the manufacture of tires, and would be expected to be worn off along with the rest of the tread during normal use.

### ***2. Review of Toxicology of Airborne Ultrafine Particles***

In fact, if the hypothesis is correct that ambient UFP are toxicologically more active than particles of the larger modes, one would expect the exposure–response relationship between adverse effects and particulate mass concentrations to be bi-phasic or curvilinear. The slope should be steeper at lower mass concentrations and flatter at higher mass concentrations when ultrafine particles are removed by heterogeneous coagulation. Coagulation of ultrafine particles onto accumulation mode particles is 10-100 times faster than homogeneous coagulation within the ultrafine mode (NRC 1979). The exposure–response relationship for daily mortality observed in the old data of the London smog episodes of the 1950’s through the 1970’s displays precisely this curvilinear form, indicating that at lower airborne mass concentrations the slope is steeper than at higher concentrations. Figure S-1 summarizes those data with respect to daily mortality observed during these episodes (Schwartz and Marcus 1990). This behavior is consistent with a greater reactivity of ultrafine particles, i.e., at lower ambient

particle mass concentrations below  $\sim 100 \mu\text{g}/\text{m}^3$  ultrafine particles persist much longer whereas at higher concentrations coagulation to the accumulation mode occurs. Maynard and Maynard (Maynard and Maynard 2002) provided a more detailed analysis of the London smog mortality data. They concluded that particle surface area is a better dose parameter to describe these data, emphasizing the involvement of ambient ultrafine particles, due to their larger specific surface area and the phenomenon of coagulation at higher concentrations. There may be other explanations for the curvilinear behavior, however, the ultrafine particle hypothesis is consistent with the observed data.

While epidemiological studies obviously are based on realistic ambient exposures of the species of interest (humans), they indicate primarily associations, although causality can be assumed if confounders are excluded and if plausible mechanisms can be identified. With respect to the toxicological *in vivo* studies, the use of mostly high exposure concentrations and of model particles can make it difficult to extrapolate to relevant lower environmental concentrations. Even when inhaled ambient UFP are used it seems that only artificially elevated concentrations of ambient UFP – using respective concentrators (Demokritou et al. 2002; Sioutas et al. 1999) – can induce effects in healthy subjects. Although effects of UFP were consistently observed, establishing a separate ambient air standard for UFP is still under debate. There are, though, a number of characteristics that are unique for NSP, relating to their behavior in the air and in the respiratory tract, giving them a distinctly different potential to cause adverse health effects than larger sized particles. In addition to normalizing pulmonary responses by particle surface area, normalization based on lung weight can provide additional normalization across species (Fig. S-3)

### 3. *Concepts of Nanotoxicology*

#### 3.1 Laboratory Rodent Studies

The significance of a large surface area for catalytical reactions is well known (Fig. 2); it is, therefore, quite plausible that particle surface area is an appropriate dose parameter given that cell membranes and subcellular structures interact with the surface of solid

particles rather than their mass, which results in biological/toxicological responses. Of course, this is likely to change if a particle surface is modified, due to solubility or other alteration (coating; charge) or if chemically different particles are compared. For example, 20 nm TiO<sub>2</sub> and 20 nm Al<sub>2</sub>O<sub>3</sub> particles induce both a significantly greater inflammatory response when 500 µg are administered intratracheally to the lung of rats compared to the same mass dose of larger-sized TiO<sub>2</sub> and Al<sub>2</sub>O<sub>3</sub> particles, corresponding to the larger specific surface area of the ultrafine particles. However, when the persistence of the inflammatory response was evaluated it turned out that the nano-sized TiO<sub>2</sub>-exposed animals had reached control levels much earlier than the Al<sub>2</sub>O<sub>3</sub>-exposed rats (Fig. S-3) (Oberdörster et al. 1990).

Another interesting finding of the PTFE fume studies was that rats could be adapted to these highly toxic NSP by pre-exposures for 5 minutes on each of 3 consecutive days, followed on day 4 by a 15-minute exposure. Compared to non-adapted rats, which received only clean air sham-exposures on 3 days and were then exposed together with the adapted animals to the 15-minute PTFE fume exposures, pre-exposure had induced a state of tolerance: There were no clinical signs of toxicity and no significant increases in inflammatory lung lavage parameters, such as increased lavage protein and increased lavage neutrophils, as opposed to the non-adapted rats which showed severe pulmonary inflammation and all died within 3 hours (Fig. S-4) (Johnston et al. 2000).

### 3.2 Ecotoxicological Studies:

Glutathione depletion can be an indicator of oxidative stress, and the decreased LPO in gill and liver of largemouth bass after nC<sub>60</sub> exposure could be indicative of tissue repair. Initial suppressive subtractive hybridization of pooled control fish vs. pooled 0.5 ppm fullerene-exposed largemouth bass liver mRNA (web-section Table S-2) showed some indications of an inflammatory response. Enzymes related to repair of tissues were upregulated in liver (*e.g.*, putative hepatocyte growth factor activator), supporting the tissue repair hypothesis. Genes related to an inflammation response were up-regulated (*e.g.*, Macrophage Stimulating Factor), and also immunosuppressive proteins (*e.g.*, lipocalins) were found to be upregulated, with a concomitant decrease in some

inflammatory cytokines (*e.g.*, several COX genes). Clearly the immune system was responding to fullerene-exposure. In addition, proteins important in homeostasis and metabolism were suppressed (*e.g.*, glucokinase and hexokinase; Fatty Acid Binding Protein; Warm-Temperature Acclimation Related Protein). A cytochrome P450 (CYP2K1) possibly involved in fatty acid metabolism was upregulated, and is being further studied as a potential enzyme of LPO tissue repair or fullerene metabolism. Future studies will follow up with these findings in gene expression changes.

Not all nanomaterials are bactericidal, and one must be careful to not lump all nanomaterials into the same category. For example, un-coated and peptide-wrapped (Dieckmann et al. 2003) and ssDNA-wrapped Single-Walled Carbon Nanotubes (SWNT) (Zheng et al. 2003) are not toxic to *E. coli* up to ppm levels, which are the limits of their water solubility (Dr. Rockford Draper, University of Texas, personal communication).

There are several groups of organisms that represent unique targets for nano-sized materials. Micron-sized zooplankton and larger filter-feeding organisms make up the basis of aquatic food webs, and these organisms can selectively filter particles based on both size and surface chemistry (Conova 1999). Many filtering apparatuses of filter feeders do not selectively strain items from the water, rather they take all nano-sized materials and materials of specific surface chemistries (the specific chemistries are species-dependent). Changing nanomaterial surface chemistry to make them more biocompatible could ultimately lead to selective filtering and uptake by filter feeding invertebrates such as the mole crab studied by Conova (1999). Special considerations in terms of safety assessment should be made for the ability of filter-feeding invertebrates to consume nano-sized materials, which would ultimately mobilize these materials up the food chain, including to humans. In addition, many benthic and soil invertebrates specialize in ingesting sediment and extracting organic material, and the chemistry of many nano-materials predicts that engineered nanomaterials will tend to sorb to sediments (Lecoanet et al. 2004; Lecoanet and Wiesner 2004).

Another potential target group is chlorophyll-containing organisms. More efficient solar cells are being produced based on synthetic chlorophyll donating electrons to fullerenes in a carbon paste (Kureishi et al. 1999). It is unknown whether natural

chlorophyll can also donate electrons to fullerenes, and subsequently fullerenes may be able to deplete the organisms' ability to store energy. This, however, is very speculative and requires further research.

Web-Section Table S-3: Up- and down-regulated genes from initial largemouth bass suppressive subtractive hybridization studies, after fish were exposed to 0.5 ppm nC<sub>60</sub> for 48 hours.

some UP-regulated genes

<b>gene</b>	<b>function</b>
alpha-2-HS-glycoprotein	differentiation of monocytes and macrophages
AMBP protein precursor	is a lipocalin with immunosuppressive properties
complement component C5-1	classical complement pathway
CYP 2K4	oxidoreductase, on ER
fibrinogen beta chain	blood clotting
G proteins	cell signaling
heart-type fatty acid binding protein	involved in lipid metabolism; growth inhibition and differentiation
macrophage stimulating 1	similar to hepatocyte growth factor; response to inflammation; released in response to tissue damage; activates macrophages; reduces NO production (negative feedback?)
plasma hyaluronan-binding protein precursor	serine protease; possibly regulates Hepatocyte growth factor activator? regulates immune cell adhesion and activation
putative hepatocyte growth factor activator (GRAAL)	regeneration of tissue damage; activated by thrombin in tissues; regulated by serine proteases
similar to 4-hydroxyphenylpyruvate dioxygenase	oxido-reductase; Catalysis of the reaction: 4-hydroxyphenylpyruvate + O <sub>2</sub> = homogentisate + CO <sub>2</sub> .

some DOWN-regulated genes

<b>gene</b>	<b>function</b>
alpha-2-macroglobulin-2	a plasma proteinase inhibitor; a member of the complement family of serum proteins; may also function as a potent adjuvant in eliciting immune responses; potent immune enhancement
apolipoprotein A1 precursor	Apolipoprotein (apo) A1 plays a central role in the metabolism of HDL
apolipoprotein H	defense/immunity; heparin

	binding
chemotaxin	activates macrophages
complement component C3	immune system opsonin
cytochrome c oxidase subunit II (COX 2)	reduction of O <sub>2</sub> ; involved in inflammatory pathway
differentially regulated trout protein	upregulation of immune response
elastase 4 precursor	Polymorphonuclear (PMN) granulocytes contain elastase 4; PMN elastase in conjunction with oxyradicals can cause tissue damage; elastase is a proteolytic enzyme that is used by PMNs to destroy invaders
fatty acid binding protein-2, hepatic	involved in lipid metabolism; growth inhibition and differentiation
ferritin, middle subunit	iron storage
glucokinase	Catalysis of the reaction: ATP + D-glucose = ADP + D-glucose 6-phosphate; critical role in sensing hypoglycemia; control of glucose metabolism
hepcidin precursor	innate immune system as anti-microbial agent; iron absorption
organic solute transporter beta	estrone 3-sulfate transport activity; inhibited by anionic drugs; also transports taurocholate, digoxin, and prostaglandin E2 but not of estradiol 17beta-d-glucuronide or p-aminohippurate
prostaglandin D synthase	role of regulating body temperature and also promotes wakening; glutathione-dependent; role in reproduction
related to verrucotoxin-□	haemolysis, hypotensive and cytolytic factor
ribosomal protein L26	expressed during anoxia; stabilizes mRNA
saxitoxin and tetrodotoxin binding protein 1 precursor	glycoprotein; involved in accumulation and/or excretion of toxins in puffer fish.
warm-temperature-acclimation-related-65kDa-protein	acclimation response

### 3.3 ROS Mechanisms of Nano-Sized Particle Toxicity

### 3.4 Exposure-Dose-Response Considerations

## **4. Portals of Entry and Target Tissues**

### 4.1 Respiratory Tract

The ICRP model predictions are based on experimental evidence of numerous well-conducted studies in humans for particles above 0.1  $\mu\text{m}$  for all three regions of the respiratory tract (for review see EPA 1996). With respect to NSP, experimental data for nasal deposition in humans have been published (Cheng et al. 1996; Swift et al. 1992) which served as a basis for the ICRP model shown in Figure 8. There are also deposition data for inhaled NSP in humans for tracheobronchial and the alveolar region of the respiratory tract (Jaques and Kim 2000), and there are human deposition data for total respiratory tract deposition (Daigle et al. 2003; Jaques and Kim 2000; Schiller et al. 1988). All of these agree reasonably well with the ICRP model. Additional experimental data for deposition of particle sizes below 50 nm in the human tracheobronchial and alveolar regions are still needed. However, since the predictions of the ICRP (1994) and other models are based on experimental data from several groups using most of the different particle sizes, as well as on validated mathematical descriptions of a particle's inertial, gravimetric and diffusional behavior in anatomical replicas, these models are well accepted and widely used for dosimetric purposes.

The information about the fraction of inhaled particles depositing in different regions of the respiratory tract provided in Figure 8 should not be misinterpreted by assuming that a high deposition fraction in one region of the respiratory tract also implies a high dose to individual cells in that region. Considering the large differences in epithelial surface area between the different regions, just the opposite could be true. For example, inhaled 20 nm particles are predicted to have the highest deposition efficiency in the alveolar region of the lung. When modeling the deposition of such particles along the individual generations of the lower respiratory tract, one can see that most of the mass of these particles is depositing beyond generation 16 of the tracheobronchial region, *i.e.*, in the alveolar region (Fig. S-5a). However, taking into account that the epithelial surface areas in tracheobronchial and alveolar regions have vastly different sizes, the

deposited dose normalized per unit surface area or per cell is quite different. Figure S-5b shows that in that case, the upper generations of the tracheobronchial region receive the highest doses per unit surface area. An additional factor that needs to be considered is that during deposition hot spots of deposition occur at bifurcational junctions (Balásházy et al. 1999, 2003). These hot spots comprising about 100 cells or areas of  $100 \times 100 \mu\text{m}$  on cranial ridges, can increase focal concentrations by 1-2 orders of magnitude.

An example may serve to illuminate further differences between regional and surface area deposition, by comparing the predicted deposition of inhaled poly-disperse ultrafine (CMD 20 nm) and fine (CMD 250 nm) particles in the three regions of the human respiratory tract during nose breathing (Figure S-5). Assumed is an inhaled concentration of  $100 \mu\text{g}/\text{m}^3$  over a 6-hr. exposure period. The geometric standard deviation of the particle size distribution is 1.7. Deposited amounts, or dose, per region and per unit surface area in all three regions of the respiratory tract are shown, as predicted by a Multiple Path Particle Deposition (MPPD) model (Asgharian et al. 1999). The dose deposited per region increases from the nasal to the tracheobronchial to the alveolar region for both particle sizes. However, the ultrafine particle deposition on a mass basis is more than twice in each of the three regions compared to the fine particles. When expressing the deposited dose per unit surface area, a different picture emerges. While the more than 2-fold greater deposition of the ultrafine aerosol is unchanged, the highest surface area dose is now received by the naso-pharyngeal area followed by the tracheobronchial region, and the least is deposited in the alveolar region (Figure S-5). Expressed in terms of number of particles per unit surface area, it is about 5,000 times higher for the ultrafine particles compared to the fine particles. This may have significant implications for the likelihood of NSP to cause effects and to be translocated to extrapulmonary sites as will be discussed in the section 4.1.2.

#### 4.1.1 Efficient Deposition of Inhaled Nano-Sized Particles

#### 4.1.2 Disposition of NSP in the Respiratory Tract

##### Classical Clearance Pathways

Nasal mucosa and tracheobronchial region are supplied with an effective clearance mechanism consisting of ciliated cells forming a mucociliary escalator to move a mucus blanket towards the pharynx (posterior nasal region and tracheobronchial region). This constitutes a very fast clearance for solid particles which, in the tracheobronchial region, removes most of them within 24 hours. It operates most likely also for deposited ultrafine particles (Kreyling et al. 2002). Studies by Schürch et al. (1990) show, however, that surface tension lowering forces of a thin surfactant layer in the bronchial tree act on particles to submerge them into the mucus and sol phase of the airway fluid which may result in a prolonged retention of particles in this region as observed by Stahlhofen et al. (1995). From the oropharynx, particles are then swallowed into the GI tract thus being eliminated from the respiratory tract. A more detailed review of these mechanisms is provided by Kreyling and Scheuch (2000).

The involvement of different surface receptors for particle phagocytosis by alveolar macrophages and subsequent events of macrophage activation and cytokine and chemokine release have been reviewed elsewhere (Dörger et al. 2000; Valberg and Blanchard 1991).

The results from the study of macrophage lavage recovery of NSP vs. larger sized particles imply that NSP – inhaled and deposited as singlets in the alveolar space – are not efficiently phagocytized by alveolar macrophages. This could be either due to an inability of macrophages to phagocytize these small particles; or due to a lack of the deposited singlet NSP to generate a chemotactic signal at the site of their deposition, or caused by surfactant action facilitating epithelial cell uptake. Studies supporting the first hypothesis show that an optimal particle size for phagocytosis by alveolar and other macrophages is between 1-3  $\mu\text{m}$ , and that beyond these sizes phagocytosis rates become progressively slower (Green et al. 1998; Hahn et al. 1977; Tabata and Ikada 1988). However, *in vitro* dosing of alveolar macrophages with ultrafine particles indicates that they are phagocytized by macrophages and activate these cells (Brown et al. 2001; Donaldson et al. 2002; Li et al. 2003; Stone et al. 1998), and it has been shown that macrophages can sense nano-scale grooves down to a depth of 71 nm under cell culture conditions (Wojciak-Stothard et al. 1996). Obviously, *in vitro* studies using monolayers of alveolar macrophages or macrophage cell-lines with direct application of the particles

onto the cells do not mimic realistic *in vivo* conditions, a chemotactic gradient is not needed in a dense cell culture to encounter the particles. However, one can safely assume that, even if the phagocytosis rate for NSP is much slower, internalization would have occurred by 24 hours post-deposition *in vivo*, provided the alveolar macrophages came into contact with the deposited NSP. Therefore, the second and third hypotheses are more likely to explain the result in Figure 10, that the macrophages do not “sense” the deposited NP since they do not generate a chemotactic signal or only a very weak one, and that the alveolar epithelial surfactant layer accelerates contact of the particles with epithelial cells (Schürch et al., 1990). This suggestion is also supported by the low deposited dose per unit alveolar surface area even for the 20 nm ultrafine particles which have the highest deposition efficiency there (Fig. S-5b). Still, experimental proof for this hypothesis is needed to explain the results of Figure 10 that only a low percentage of NSP deposited by inhalation in the alveolar region is taken up by alveolar macrophages.

#### Epithelial Translocation

Since the different particle types had been intratracheally instilled as aggregates rather than inhaled as singlet particles, the authors suggested that i) TiO<sub>2</sub> in contrast to carbon black disaggregated to a greater degree than carbon black which led to endocytosis into epithelial cells and translocation to the pulmonary interstitium; or ii) that the large interstitial dose gave rise to a shift of the inflammatory response (chemotactic stimuli) from the alveolar space to the interstitium such that elicited inflammatory neutrophils were not attracted into the alveolar space. No histological examination of the lung tissue was performed to confirm the shift of inflammation towards the interstitium. However, earlier as well as later studies substantiated the propensity of NSP to translocate across epithelial layers and reach remote extrapulmonary sites (see section 4.2).

In general, interstitial translocation constitutes a translocation pathway for those particles which are not phagocytized by alveolar macrophages, either due to their small size – as is the case for NSP – or due to an overloading of the alveolar macrophage capacity to phagocytize particles. A state of particle overload has been induced in a number of chronic rat inhalation studies with very high particle concentrations leading to

increased translocation of the larger fine particles into the interstitium (ILSI 2000). Once in the interstitium, translocation to regional lymph nodes can occur either as free particles or after phagocytosis by interstitial macrophages. Some engineered NP, specifically fullerene derivatives, have been shown to be antigenic (Braden et al. 2000; Chen et al. 1998; Erlanger et al. 2001), raising the possibility of humoral immune responses after exposure to these NP. It is unknown at this point whether other NP are also antigenic.

Translocation to regional lymph nodes of larger-sized, respirable, poorly soluble particles in a particle overload situation is a well-known phenomenon. However, such translocation occurs with NSP at much lower lung doses expressed as mass. NSP accumulation in the local lymph nodes is even more pronounced in a situation where exposure to these particles results in higher lung burdens. This was seen in a study in which rats were exposed for 12 weeks to high concentrations of ultrafine (20 nm) or fine (250 nm) TiO<sub>2</sub> particles. TiO<sub>2</sub> lung burdens as well as TiO<sub>2</sub> content in bifurcational lymph nodes were determined at the end of exposure and 7 months post-exposure (Oberdörster et al. 1994). Because of the high exposure concentration of ~20 mg/m<sup>3</sup>, the ultrafine particles as well as the fine particles were inhaled as aggregates with similar aerodynamic diameter of 0.7 – 0.8 μm which resulted in similar deposition of both particle types throughout the respiratory tract. As was found in prior studies (Fig. 5a,b), the inflammatory response with concomitant increase in alveolar neutrophil numbers was much greater for ultrafine TiO<sub>2</sub> and correlated with the larger particle surface area. There is evidence that disaggregation of the aggregated ultrafine TiO<sub>2</sub> particles occurred which facilitated translocation across alveolar epithelium and to regional lymph nodes. Subsequently, there was an almost 6-fold higher accumulation of ultrafine TiO<sub>2</sub> in the regional thoracic lymph nodes compared to the fine TiO<sub>2</sub> by mass.

#### Translocation to the Circulatory System

Some particles after accumulation in lymph nodes will also translocate further into post-nodal lymph and enter the blood circulation. This mechanism was demonstrated for fibrous particles in dogs: Intrabronchially instilled amosite fibers were found in post-nodal lymph samples of the right thoracic duct collected in the neck area before entering the venous circulation (Oberdörster et al. 1988). There was an obvious

size limitation in that only the shorter and thinner fibers (< 500 nm diameter) appeared in the post-nodal lymph. A lympho-hematogeneous pathway was also suggested in non-human primates to explain the translocation of fine crystalline silica particles to the livers of exposed monkeys, following chronic inhalation of high concentrations (Rosenbruch 1990; Rosenbruch and Krombach 1992). Thus, the clearance pathway from local lymph nodes to the blood circulation is not restricted to NSP but occurs also for fine particles, although rates are likely different. The initial step, however, involving transcytosis across the alveolar epithelium into the pulmonary interstitium, seems to occur with larger particles only under high lung load situations or with cytotoxic particles (*e.g.*, crystalline SiO<sub>2</sub>) when the phagocytic capacity of alveolar macrophages is overwhelmed and the particles are present in the alveoli as free particles for an extended period of time.

Several recent studies in rodents and humans indicate that rapid translocation of inhaled NSP into the blood circulation occurs. Nemmar et al. (2002) reported findings in humans that inhalation of <sup>99m</sup>Tc-labelled ultrafine carbon particles (Technegas<sup>®</sup>) resulted in the rapid appearance of the label in the blood circulation shortly after exposure and also in the liver. They suggested that this at least partly indicated translocation of these particles into the blood circulation. In contrast, other studies in humans with <sup>99m</sup>Tc-labeled carbon particles (33 nm) by Brown et al. (2002) did not confirm such uptake into the liver, and the authors cautioned that the findings by Nemmar et al. (2002) were likely due to soluble pertechnetate rather than labeled ultrafine particles. Inhalation studies in rats have shown that ultrafine elemental <sup>13</sup>C particles (CMD ~30 nm) had accumulated to a large degree in the liver of rats by 24 hours after exposure, indicating efficient translocation into the blood circulation (Oberdörster et al. 2002). These NSP were generated in an argon atmosphere by electric spark discharge between two elemental <sup>13</sup>C electrodes, with subsequent addition of diluting air. Suggested pathways into the blood could be across the alveolar epithelium as well as across intestinal epithelium from particles cleared via the mucociliary escalator and swallowed into the GI tract. On the other hand, using a method of intratracheal inhalation of ultrafine <sup>192</sup>Ir particles in rats, Kreyling et al. (2002) found only minimal translocation (<1%) from the lung to extrapulmonary organs, although they reported 10-fold greater translocation of the smaller (15 nm) compared to the larger (80 nm) ultrafine particles. As an explanation for

the apparent difference between the behavior of ultrafine iridium and carbon particles the authors discuss the possibility of their binding to proteins which may either facilitate or impede translocation across epithelia.

The conclusion from these studies is that translocation of inhaled NSP from the respiratory tract into the blood circulation can occur, although the efficiency of such translocation may well depend on the chemical and surface characteristics of the particles. Kato et al. (2003) reported in a most recent study in rats that even particles as large as 240 nm translocated from the alveoli into intravascular spaces by transcytosis across Type I and Type II cells, provided the particles were coated with lecithin, which indicates that surface properties may play a crucial role. It is conceivable that differences in surface coating of the aforementioned studies with nano-sized elemental  $^{13}\text{C}$  and  $^{192}\text{Ir}$  can account for the observed differences to translocate: Most recent analyses about the chemical composition of the electric spark discharge generated  $^{13}\text{C}$  particles revealed that they have a coating of organics, most likely coming from impurities of the diluting air, which adsorb on the large surface area of the particles (Su et al. 2004). Additional studies are needed to determine particle size and surface chemistry dependent translocation rates across the alveolar epithelial/endothelial cell barrier.

The results of Nemmar et al. (2002; 2003) provide further indirect evidence that NSP are translocating from the lung into the blood circulation and affect blood coagulation. These authors saw in an experimental thrombosis model in hamsters that *i.v.* injected and intratracheally instilled positively, but not negatively, charged 60 nm polystyrene particles accelerated thrombus formation acutely in a peripheral vein. Larger 400 nm positively charged particles did not increase acute thrombus formation when intratracheally instilled at a dose which induced pulmonary inflammation equivalent to the dose of thrombus-inducing 60 nm particles. Although high doses were used, these results are consistent with the concept that *i*) nano-sized but not fine particles deposited in the lung translocate to the blood circulation and can affect endothelial function; *ii*) that surface properties – including charge and also chemistry (Kato et al. 2003; Oberdörster et al. 2000) – are important determinants of effects of NSP.

Caveolae existing in alveolar epithelial and endothelial cell membranes (Oberdörster and Utell 2002) mediate translocation as discussed above, but also clathrin-

coated pits may be involved. Virologists have investigated the various modes that viruses (biological NSP) gain entry into cells and interact with cytoskeletal and other subcellular structures during their intracellular pathways (Bantel-Schaal et al. 2002; Helenius et al. 1980; Lakadamyali et al. 2003; Pelkmans et al. 2001; Seisenberger et al. 2001; Suomalainen et al. 1999). A recent review (Smith and Helenius 2004) summarizes these processes of endocytosis and intracellular distribution. Receptors and Attachment Factors are the first lines of interaction between viruses and cells, after which viruses are endocytosed and “given a free ride deep into the cytoplasm”. Endocytosis is mediated *via* clathrin-coated pits or *via* caveolae, followed by transport of the virus particle into the cytoplasm and ultimately into the nucleus, which has a 39 nm nuclear pore size. These simple mechanisms require no macromolecular assemblies to pass the nano-sized particle (virus) through the plasma membrane to the nucleus. Based on the studies summarized in Table 4, these endocytotic pathways are very likely also operational for NP, dependent on surface properties as discussed.

#### Neuronal Uptake and Translocation

Day 1 <sup>13</sup>C concentrations of cerebrum and cerebellum were also significantly increased, but the increase was inconsistent, significant only on one additional day of the post-exposure period, possibly reflecting translocation across the blood-brain barrier in certain brain regions. The increases in olfactory bulbs are consistent with the earlier studies in non-human primates which had demonstrated that intranasally-instilled solid NSP translocate along axons of the olfactory nerve into the CNS. These studies demonstrated that the CNS can be targeted by airborne solid NSP and that the most likely mechanism is translocation from deposits on the olfactory mucosa of the nasopharyngeal region of the respiratory tract *via* the olfactory nerve.

Translocation of NSP from airway mucosa along sensory nerves in non-human primates and rodents is little recognized as a mechanism of importance in the area of health effects of inhaled particles. Questions about the relevance for humans and about underlying mechanisms of neuronal uptake and transport arise. Figure 13 shows schematically the gross and fine anatomical structure of the human olfactory mucosa with olfactory neuronal dendrites and axons and its proximity to the olfactory bulb of the

brain. It has been well demonstrated in rodents in numerous studies that inhaled or intranasally instilled soluble metal compounds are translocating *via* olfactory neurons to the olfactory bulb (Brenneman et al. 2000; Dorman et al. 2002; Gianutsos et al. 1997; Tjälve and Henriksson 1999). Dorman et al. (2002) pointed out the importance of solubility for the translocation of inhaled Mn compounds along the olfactory route. Significantly less Mn from inhaled poorly soluble 1.6  $\mu\text{m}$  Mn-phosphate particles compared to soluble Mn-sulfate accumulated in the olfactory bulb of rats. The large particle size of 1.6  $\mu\text{m}$  ruled out neuronal translocation as solid particles. The olfactory nerve pathway has also been demonstrated in fish using soluble Mn (Tjälve et al. 1995), and could have played a role in fullerene-induced Lipid Peroxidation in largemouth bass brain described in section 3.2 (Oberdörster 2004).

The following comparison between rats and humans is an attempt to quantify the human CNS exposure from inhaled NSP *via* the olfactory neuronal pathway using data from the rat study with inhaled nano-sized carbon  $^{13}\text{C}$ . From the results of this study, it was estimated that  $\sim 20\%$  of the deposited amount translocated to the olfactory bulb within 7 days after the exposure (Oberdörster et al. 2004). The airflow directed to the human nasal olfactory mucosa (5% of total nasal mucosa) is 10% of the total nasal airflow (Keyhani et al. 1997). A much larger relative olfactory mucosa of 50% of the nasal mucosa in the rat receives only 15% of the total nasal airflow (Kimbell et al. 1997), so that the relative deposited amount per unit surface area of the olfactory mucosa may be not that different between rats and humans. Indeed, the Multiple Path Particle Deposition (MPPD) model (Asgharian et al. 1999) predicts that deposition of inhaled 20 nm particles in the nasopharyngeal region is about 5 times greater per unit nasal surface area in humans than in rats, *i.e.*,  $\sim 60 \text{ ng/cm}^2$  for rats compared to  $\sim 300 \text{ ng/cm}^2$  in humans, assuming a 6-hr. exposure at  $100 \mu\text{g/m}^3$  under normal resting breathing conditions for both species. Assuming even distribution across the nasal mucosa – which is most likely not quite correct – rats would deposit  $\sim 480 \text{ ng}$  on their olfactory mucosa and humans about  $\sim 1,575 \text{ ng}$ . Using the 20% translocation value estimated in the  $^{13}\text{C}$  translocation study, the rats would translocate 96 ng to their olfactory bulbs (85 mg organ weight), and humans would translocate 315 ng to their olfactory bulbs (168 mg organ weight (Turetsky et al. 2003); that is 1.1 ng/mg olfactory bulb in rats and 1.9 ng/mg olfactory

bulb in humans, a 1.6-fold higher concentration in humans. This is a rough estimate only and should not be over-interpreted and generalized for all NSP since neuronal translocation rates may be very dependent on particle size, surface chemistry and other parameters, and may also be different between rodents and humans.

If – instead of assuming even distribution of deposited NSP – one takes a different approach and assumes that inhaled 20 nm particles are depositing on the olfactory mucosa proportionately to the airflow directed to that region, the result changes even more towards a higher surface area dose in the human olfactory mucosa and a lower one in rats. In rats it would be 20 ng/cm<sup>2</sup> (160 ng on total olfactory mucosa), and in humans 600 ng/cm<sup>2</sup> (3150 ng on total olfactory mucosa), a 30-fold difference. The olfactory bulb would then be dosed with 32 ng in rats and 630 ng in humans (20% translocation of deposited amount), equivalent to olfactory bulb concentrations of 0.4 ng/mg in rats and 3.8 ng/mg in humans, an almost 10-fold higher concentration in humans.

Of course, these modeling exercises do not prove that efficient olfactory translocation of inhaled NSP in humans occurs, but the evidence in non-human primates including chimpanzees strongly support the existence of this mechanism in humans despite a rudimentary olfaction system; and the dosimetric calculations indicate that this pathway could be significant, especially considering accumulations during repeated, even low level, exposures to airborne NSP. Final confirmation of nano-sized particle neuronal translocation obviously can only come from human evidence. Even if the surface loading of the human olfactory mucosa is much less than the model predicts, and therefore the amount being translocated is much less, an exposure over many years or decades conceivably could result in significant accumulation of biopersistent nano-size particles in the olfactory bulb.

The chemistry of ambient UFP depend on particle size and source of origin. The smaller ambient ultrafine particles approaching 10 nm consist increasingly of organic compounds (Kittelson 1998) which are lipid or water soluble. It is conceivable that these, too, could be translocated *via* neurons since neuronal transport of proteins, lipids, and cellular organelles is a well known phenomenon (Grafstein and Forman 1980). A likely mechanism for neuronal transport of solid NSP is the cell's shuttle system of axonal and dendritic microtubuli (Hirokawa 1998), involving binding proteins of the Kinesin

Superfamily. Numerous open questions are still to be answered, including questions about uptake and transport mechanisms, influence of physico-chemical properties of NSP on translocation, translocation into deeper CNS structures, adverse effects on the CNS from translocated NSP, and, most importantly, what is the extent of neuronal translocation of NSP in humans? Again, insights from virology on intracellular movements of these nano-sized viruses could guide efforts in nanotoxicology to determine intracellular and transcellular NSP movements.

Exposure to airborne NSP at certain occupational settings should also be considered in the context of CNS effects. For example, arc welding generates large number concentrations of ultrafine and fine metal oxide particles (Zimmer et al. 2002), and a recent epidemiological study suggested an increased risk of welders to develop Parkinson's Disease almost 20 years earlier than the general population (Racette et al. 2001). Manganese in welding fumes is a known neurotoxicant (Aschner 2000), and its ultrafine particle size in welding fumes could potentially facilitate translocation to the CNS. Studies in rats show efficient translocation of inhaled nano-sized Mn-oxide to the olfactory bulb in rats (Fig. 12). A link between these two findings still needs to be established in future studies.

## 4.2 GI Tract and Skin

Various viruses (biological NSP) have long been known to travel *via* neuronal pathways, including viral meningitis, herpes virus (producing cold sores), and chicken pox (producing shingles). The neuronal uptake mechanism has been described specifically for the respiratory tract, and it is not known whether it exists for other exposure routes as well. However, the same or similar translocation mechanisms may apply to dermal and intestinal exposures once penetration across the epidermis into the corium or across intestinal epithelium has occurred (see section 4.2).

### 4.2.2 Epithelial Translocation

Instilled doses ranged from 65  $\mu\text{g}$  to 1000  $\mu\text{g}$ , yet the highest doses – in terms of particle surface area retained in the lung – resulted in fewer inflammatory neutrophils in the lung lavage (Figure 7a). In contrast, a similarly high dose (in terms of particle surface) of 20 nm carbon black showed the expected greater response at higher doses.

On the other hand, lung lavage protein – another inflammatory indicator for increased epithelial permeability – showed a steady dose dependent increase for all TiO<sub>2</sub> sizes as well as carbon black as would have been expected (Figure 7b). An additional finding was a particle size and dose dependent translocation for TiO<sub>2</sub> towards the pulmonary interstitium, whereas such translocation was only minimal for carbon black by 24 hours post-dosing (Figure 7c,d). Indeed, at the highest doses of the 12 and 20 nm TiO<sub>2</sub> about 52 and 50%, respectively, of the retained lung burden was “interstitial”, that is in epithelial or interstitial sites.

These studies with ultrafine and fine TiO<sub>2</sub> particles showed a strongly particle size dependent translocation to epithelial and interstitial sites: 24 hours after intratracheal instillation of 500 µg into rats, more than 50% of the 12 nm sized TiO<sub>2</sub> had translocated, whereas it was only 4% and less for 220 nm and 250 nm TiO<sub>2</sub> (Figure 7d).

## **5. Risk Assessment**

## **6. Summary & Outlook**

Numerous anthropogenic — mainly combustion related — and natural sources generate airborne ultrafine particulate matter (<100 nm). The ubiquitous occurrence of the ultrafine particles results in significant human exposures under environmental and certain occupational conditions. Several epidemiological studies have found adverse respiratory and cardiovascular health effects in susceptible parts of the population to be associated with these particles. Controlled clinical studies with 10-50 µg/m<sup>3</sup> ultrafine elemental carbon particles as surrogates for ambient particles did induce cardiovascular effects in healthy adults. Studies in rodent models of a compromised respiratory or cardiovascular system also showed mild inflammatory effects and oxidative stress systemically and in the respiratory tract, using either laboratory-generated ultrafine particles at high concentrations or ambient ultrafine particles. In addition, high dose *in vitro* studies confirmed that the likely mechanism for their effects is *via* induction of oxidative stress. Collectively, these results show that inhaled ambient ultrafine particles can elicit significant effects.

Lacking, however, are long-term exposure studies and additional data about short-term effects of ambient ultrafine particles at realistic concentrations. Inhaled ultrafine particles deposit in all three regions of the respiratory tract *via* diffusional processes, with the nose being a very effective filter and deposition site for the smallest (<5 nm) NSP, and tracheobronchial and alveolar regions being mainly targeted by about 5 and 20 nm particles, respectively. Once deposited, the disposition of these particles appears to be unique: In addition to the classical clearance processes known to exist for fine and coarse particles, solid NSP can translocate to extrapulmonary organs across epithelial layers and also are taken up *via* sensory nerve endings in the nasal and tracheobronchial regions. Particularly, translocation of nasally-deposited NSP along olfactory nerve axons into the olfactory bulb has been demonstrated in non-human primates and rodents, thereby circumventing the tight blood-brain barrier for accessing CNS structures. Depending on their chemical composition and bioavailability of particle components to neuronal cells, it is conceivable that NSP reaching the CNS *via* this neuronal pathway will cause adverse effects. Although this pathway is likely to exist in humans as well, conclusive evidence is still lacking. Thus, there is a need to determine the potential of airborne NSP to cause adverse CNS effects in laboratory animals and in humans. Figure S-8 summarizes hypotheses underlying effects caused by ambient ultrafine particulate matter, including systemic acute phase responses induced by alveolar inflammation or through particles reaching the blood circulation leading directly to cardiovascular effects; indirect cardiovascular effects *via* the autonomic nervous system from neuronally translocated particles to respective ganglia and CNS structures; and potentially direct effects of translocated NSP on CNS functions. Modifying factors for these events most likely include age, underlying disease and other co-airpollutants.

Although some of these emerging principles of nano-toxicology are specific for exposure *via* the respiratory tract (*e.g.*, deposition of airborne NP), the fate and effects of nanoparticles once taken up into the organism by varying routes are likely to be governed by the same mechanisms. For example, following inhalation exposure, local portal of entry effects as well as effects in extrapulmonary organs (*e.g.*, cardiovascular, liver, CNS) due to the propensity of nano-sized particles to translocate, can be expected depending on modifying particle parameters.

Specific examples of translocation and effects of nano-sized particles and presumed mechanisms are highlighted in this manuscript. They illustrate, on the one hand, that we need to be aware of possible acute adverse effects and potential long-term consequences from nanoparticle exposures; on the other hand, the findings also give us insights about the intriguing possibilities that engineered nanoparticles offer for potential use as diagnostic tools or as therapeutic delivery systems. Obviously, a thorough evaluation of desirable *vs.* adverse effects is required for the safe use of engineered nanoparticles. Thus, major challenges lie ahead to answer key questions of nanotoxicology in order to characterize and predict potential risks, foremost being the assessment of human and environmental exposure, the identification of potential short and long-term hazards. Furthermore, it is essential to understand more about the biopersistence in cells and subcellular structures, the correlation between physicochemical and biological/toxicological properties, and defining and characterizing the biokinetics of nanoparticles (*i.e.*, translocation pathways to sensitive structures within organs, mechanisms of uptake and translocation at the organ/cellular/molecular levels) as well as environmental effects such as persistence of coatings or covalent modifications under weathering (UV, microbial degradation *etc.*), potential for bioaccumulation by benthic fauna or filter feeders, and potential movement through the food chain. Research to obtain answers to these questions requires an interdisciplinary team approach involving toxicology, materials science, medicine, molecular biology, bioinformatics and their subspecialties.

## **7. References for web section**

- Aschner M. 2000. Manganese: brain transport and emerging research needs. *Environmental Health Perspectives* 108(Supplement 3):429-432.
- Asgharian B, Miller F, Subramaniam rP. 1999. Dosimetry software to predict particle deposition in humans and rats. *CIIT Activities* 19(No. 3).
- Balásházy I, Hofmann W, Heistracher T. 1999. Computation of local enhancement factors for the quantification of particle deposition patterns in airway bifurcations. *J Aerosol Science* 30(No. 2):185-203.
- Balásházy I, Hofmann W, Heistracher T. 2003. Local particle deposition patterns may play a key role in the development of lung cancer. *Journal of Applied Physiology* 94:1719-1725.

- Bantel-Schaal U, Hub B, Kartenbeck J. 2002. Endocytosis of adeno-associated virus type 5 leads to accumulation of virus particles in the Golgi Compartment. *J Virology* 76(5):2340-2349.
- Berry JP, Arnoux B, Stanislas G, Galle P, Chretien J. 1977. A microanalytic study of particles transport across the alveoli: Role of blood platelets. *Biomedicine* 27:354-357.
- Bracco D, Favre J-B. 1998. Pulmonary injury after ski wax inhalation exposure. *Annals of Emergency Medicine* 32(5):616-619.
- Braden B, Goldbaum F, Chen B, Kirschner A, Wilson S, Erlanger B. 2000. X-ray crystal structure of an anti-Buckminsterfullerene antibody Fab fragment: Biomolecular recognition of C60. *PNAS* 97(22):12193-12197.
- Brenneman KA, Wong BA, Buccellato MA, Costa ER, Gross EA, Dorman DC. 2000. Direct olfactory transport of inhaled manganese ( $^{54}\text{MnCl}_2$ ) to the rat brain: Toxicokinetic investigations in a unilateral nasal occlusion model. *Toxicol Appl Pharmacol* 169:238-248.
- Brown DM, Wilson MR, MacNee W, Stone V, Donaldson K. 2001. Size-dependent proinflammatory effects of ultrafine polystyrene particles: A role for surface area and oxidative stress in the enhanced activity of ultrafines. *Toxicology and Applied Pharmacology* 175:191-199.
- Brown JS, Zeman KL, Bennett WD. 2002. Ultrafine particle deposition and clearance in the healthy and obstructed lung. *Am J Respir Crit Care Med* 166:1240-1247.
- Cass GR, Hughes LA, Bhave P, Kleeman MJ, Allen JO, Salmon LG. 2000. The chemical composition of atmospheric ultrafine particles. *Phil trans R Soc Lond A* 358:2581-2592.
- Chang OMC, Yi S-MY, Hopke PK, England GC, Chow JC, Watson JG. in press. Measurement of ultrafine particle size distributions from stationary combustion sources of coal, oil, and gas. *J of the Air & Waste Management Association* 00(00):00-00.
- Chen B, Wilson S, Das M, Coughlin D, Erlanger B. 1998. Antigenicity of fullerenes: Antibodies specific for fullerenes and their characteristics. *PNAS* 95:10809-10813.
- Cheng YS, Yeh HC, Guilmette RA, Simpson SQ, Cheng KH, Swift DL. 1996. Nasal deposition of ultrafine particles in human volunteers and its relationship to airway geometry. *Aerosol Science & Technology* 25:274-291.
- Conova S. 1999. Role of particle wettability in capture by suspension-feeding crab (*Emerita talpoida*). *Marine Biology* 133:419-428.
- Dahlquist M, Alexandersson R, Andersson K, Kolmodin-Hedman B, Malker H. 1992. Exposure to ski-wax smoke and health effects in ski waxers. *ApplOccupEnvironHyg* 7(10):689-693.
- Daigle CC, Chalupa DC, Gibb FR, *et al.* 2003. Ultrafine particle deposition in humans during rest and exercise. *Inhalation Toxicology* 15(No. 6):539-552.
- deLorenzo A. 1970. The olfactory neuron and the blood-brain barrier. In: Taste and smell in vertebrates (Wolstenholme G, Knight J, eds). London:J. & A. Churchill, 151-176.
- Demokritou P, Gupta T, Koutrakis P. 2002. A high volume apparatus for the condensational growth of ultrafine particles for inhalation toxicological studies.

- Aerosol Science and Technology 36:1061-1072.
- Dieckmann G, Dalton A, Johnson P, *et al.* 2003. Controlled assembly of carbon nanotubes by designed amphiphilic Peptide helices. *J Am Chem Soc* 125(7):1770-1777.
- Donaldson K, Brown D, clouter A, *et al.* 2002. The pulmonary toxicology of ultrafine particles. *J Aerosol Medicine - Deposition Clearance & Effects in the Lung* 15(2):213-220.
- Dörger M, Münzing S, Allmeling A-M, Krombach F. 2000. Comparison of the phagocytic response of rat and hamster alveolar macrophages to man-made vitreous fibers in vitro. *Human & Experimental Toxicology* 19:635-640.
- Dorman DC, Brennehan KA, McElveen AM, Lynch SE, Roberts KC, Wong BA. 2002. Olfactory transport: A direct route of delivery of inhaled manganese phosphate to the rat brain. *J Toxicology & Environmental Health (Part A: Current Issues)* 65(No. 20):1493-1511.
- EPA. 1996. Air quality criteria for particulate matter (Vol. III) 600/P-95-001cF. Washington, DC 20460: Office of Research and Development.
- Erlanger B, Chen B, Zhu M, Brus L. 2001. Binding of an anti-fullerene IgG monoclonal antibody to single wall carbon nanotubes. *Nano Letters* 1(9):465-467.
- Gianutsos G, Morrow GR, Morris JB. 1997. Accumulation of manganese in rat brain following intranasal administration. *Fundamental and Applied Toxicology* 37(Article No. FA972306):102-105.
- Grafstein B, Forman DS. 1980. INTRACELLULAR TRANSPORT IN NEURONS. *Physiological Reviews* 60(NO. 4):1167-1283.
- Green TR, Fisher J, Stone M, Wroblewski BM, Ingham E. 1998. Polyethylene particles of a "critical size" are necessary for the induction of cytokines by macrophages in vitro. *Biomaterials* 19:2297-2302.
- Hahn FF, Newton GJ, Bryant PL. 1977. In vitro phagocytosis of respirable-sized monodisperse particles by alveolar macrophages. In: *Pulmonary Macrophages and Epithelial Cells* (Sanders CL, Schneider RP, Dagle GE, Ragen HA, eds):ERDA Symposium Series, 424-435.
- Helenius A, Kartenbeck J, Simons K, Fries E. 1980. On the entry of semliki forest virus into BHK-21 cells. *J Cell Biol* 84:404-420.
- Hirokawa N. 1998. Kinesin and dynein superfamily proteins and the mechanism of organelle transport. *Science* 279:519-526.
- ICRP. 1994. Human Respiratory Model for Radiological Protection. *Annals of the ICRP* 24:ICRP publication # 66.
- ILSI. 2000. ILSI Risk Science Institute Workshop: The relevance of the rat lung response to particle overload for human risk assessment: A workshop consensus report (ILSI risk Science Inst. Workshop Participants). *Inhalation Toxicology* 12(Nos. 1-2):1-17.
- Jaques PA, Kim CS. 2000. Measurement of Total Lung Deposition of Inhaled Ultrafine Particles in Healthy Men and Women. *Inhalation Toxicology* 12:715-731.
- Johnston CJ, Mango GW, Finkelstein JN, Barry BR. 1997. Altered pulmonary response to hyperoxia in Clara cell secretory protein deficient mice. *American Journal Respiratory Cell Molecular Biology* 17:147-155.
- Johnston CJ, Finkelstein JN, Mercer P, Corson N, Gelein R, Oberdorster G. 2000.

- Pulmonary effects induced by ultrafine PTFE particles. *Toxicol Appl Pharmacol* 168:208-215.
- Kato T, Yashiro T, Murata Y, *et al.* 2003. Evidence that exogenous substances can be phagocytized by alveolar epithelial cells and transported into blood capillaries. *Cell Tissue Research* 311:47-51.
- Keyhani K, Scherer PW, Mozell MM. 1997. A numerical model of nasal odorant transport for the analysis of human olfaction. *J theor Biol* 186:279-301.
- Kimbell JS, Godo MN, Gross EA, Joyner DR, Richardson RB, Morgan KT. 1997. Computer simulation of inspiratory airflow in all regions of the F344 rat nasal passages. *Toxicology & Applied Pharmacology* 145:388-398.
- Kittelson DB, Watts W, Johnson J. 2001. Fine Particle (nanoparticle) emissions on Minnesota highways.: Mn/DOT Report No. 2001-12.
- Kittelson DV. 1998. Engines and nanoparticles: A Review. 29(5,6):575-588.
- Kreyling W, Semmler M, Erbe F, *et al.* 2002. Translocation of ultrafine insoluble iridium particles from lung epithelium to extrapulmonary organs is size dependent but very low. *J Toxicology & Environmental Health* 65A(20):1513-1530.
- Kreyling WG, Scheuch G. 2000. Chapter 7: Clearance of Particles Deposited in the Lungs. In: *Particle-Lung Interactions* (Gehr P, Heyder J, eds). New York - Basel:Marcel Dekker, Inc., 323-376.
- Kureishi Y, Tamiaki H, Shiraishi H, Maruyama K. 1999. Photoinduced electron transfer from synthetic chlorophyll analogue to fullerene C60 on carbon paste electrode. Preparation of a novel solar cell. *Bioelectrochem Bioenerg* 48(1):95-100.
- Lakadamyali M, Rust M, Babcock H, Zhuang X. 2003. Visualizing infection of individual influenza viruses. *PNAS* 100:9280-9285.
- Lecoanet H, Bottero J, Wiesner M. 2004. Laboratory Assessment of the Mobility of Nanomaterials in Porous Media. *Environ Sci Technol* 38:5164-5169.
- Lecoanet H, Wiesner M. 2004. Velocity effects on fullerene and oxide nanoparticle deposition in porous media. *Environ Sci Technol* 38(16):4377-4382.
- Li N, Sioutas C, Cho A, *et al.* 2003. Ultrafine particulate pollutants induce oxidative stress and mitochondrial damage. *Environmental Health Perspectives* 111(No. 4):455-460.
- Maynard AD, Maynard RL. 2002. A derived association between ambient aerosol surface area and excess mortality using historic time series data. *Atmospheric Environment* 36:5561-5567.
- Nemmar a, Hoet PHM, Vanquickenborne B, *et al.* 2002. Passage of inhaled particles into the blood circulation in humans. *Circulation* 105:411-414.
- Nemmar A, Hoylaerts MF, Hoet PHM, Vermeylen J, Nemery B. 2003. Size effect of intratracheally instilled particles on pulmonary inflammation and vascular thrombosis. *Toxicology and Applied Pharmacology* 186:38-45.
- NNI. 2004. What is Nanotechnology? <http://www.nsf.gov/search97cgi/vtopic>.
- NRC. 1979. Airborne Particles. Subcommittee on Airborne Particles, Committee on Medical and Biologic Effects of Environmental Pollutants. Baltimore:University Park Press.
- Oberdörster E. 2004. Manufactured Nanomaterials (Fullerenes, C60) Induce Oxidative Stress in Brain of Juvenile Largemouth Bass. *Environ Health Perspect* 112(10):1058-1062.

- Oberdörster G, Morrow PE, Spurny K. 1988. Size dependent lymphatic short term clearance of amosite fibers in the lung. *Ann Occup Hyg* 32((Supplement, Inhaled Particles VI)):149-156.
- Oberdörster G, Ferin J, Finkelstein J, Wade P, Corson N. 1990. Increased pulmonary toxicity of ultrafine particles? II. Lung lavage studies. *21*:384-387.
- Oberdörster G, Ferin J, Lehnert BE. 1994. Correlation between particle size, in vivo particle persistence, and lung injury. *Environmental Health Perspectives* 102 (Suppl. 5):173-179.
- Oberdörster G, Finkelstein JN, Johnston C, *et al.* 2000. HEI Research Report: Acute Pulmonary Effects of Ultrafine Particles in Rats and Mice HEI Research Report. No. 96: Health Effects Institute.
- Oberdörster G. 2001. Pulmonary effects of inhaled ultrafine particles (Review). *Int Arch Occup Environ Health* 74:1-8.
- Oberdörster G, Sharp Z, Atudorei V, *et al.* 2002. Extrapulmonary translocation of ultrafine carbon particles following whole-body inhalation exposure of rats. *J Toxicology and Environmental Health* 65A:1531-1543.
- Oberdörster G, Utell MJ. 2002. Editorial: Is the central nervous system yet another target organ for ultrafine particles? *Environ Health Perspect* 110(No. 8):A440-A441.
- Oberdörster G, Sharp Z, atudorei V, *et al.* 2004. Translocation of inhaled ultrafine particles to the brain. *Inhalation Toxicology* 16(No. 6/7):437-445.
- Pelkmans L, Kartenbeck J, Helenius A. 2001. Caveolar endocytosis of simian virus 40 reveals a new two-step vesicular-transport pathway to the ER. *Nature Cell Biology* 3:473-483.
- Racette BA, McGee-Minnich L, Moerlein SM, Mink JW, Videen TO, Perlmutter JS. 2001. Welding-related parkinsonism. Clinical features, treatment, and pathophysiology. *Neurology* 56:8-13.
- Rosenbruch M. 1990. Experimentally induced liver granulomas after long-term inhalation of quartz in non-human primates. *132*:469-470.
- Rosenbruch M, Krombach F. 1992. Structural and functional hepatic changes after experimental long-term inhaation of silica in non-human primates. *Am Rev Respir Dis* 145(No. 4 (Intl. Conf. Suppl. - abstracts)):A91.
- Rundell KW. 2003. High levels of airborne ultrafine and fine particulate matter in indoor ice arenas. *Inhalation Toxicology* 15:237-250.
- Schiller CF, Gebhart J, Heyder J, Rudolf G, Stahlhofen W. 1988. Deposition of monodisperse insoluble aerosol partilces in the 0.005 to 0.2  $\mu\text{m}$  size range within the human respiratory tract. *Ann occup Hyg* 32(Supplement 1):41-49.
- Schürch S, Gehr P, Hof VI, Geiser M, Green F. 1990. Surfactant displaces particles toward the epithelium in airways and alveoli. *Respiration Physiology* 80:pp.17-32.
- Schwartz J, Marcus a. 1990. Mortality and air pollution in London: A time series analysis. *American Journal of Epidemiology* 131 (1):185-194.
- Seisenberger G, Ried M, Endreb T, Büning H, Hallek M, Bräuchle C. 2001. Real-time single-molecule imaging of the infection pathway of an adeno-associated virus. *Science* 294:1929-1932.
- Sioutas C, Kim S, Chang M. 1999. Development and evaluation of a prototype ultrafine particle concentrator. *JAerosol Science* 30(8):1001-1012.

- Smith AE, Helenius A. 2004. How viruses enter animal cells. *Science* 304:237-242.
- Stahlhofen W, Scheuch G, Bailey MR. 1995. Investigations of retention of inhaled particles in the human bronchial tree. *Radiation Protection Dosimetry* 60 (No. 4):311-319.
- Stone V, Shaw J, Brown D, MacNee W, Faux S, Donaldson K. 1998. The role of oxidative stress in the prolonged inhibitory effect of ultrafine carbon black on epithelial cell function. *Toxicol In Vitro* 12:649-659.
- Su Y, Sipin M, Prather K, Gelein R, Lunts A, Oberdörster G. 2004. ATOFMS characterization of individual model aerosol particles for exposure studies. *Aerosol Science and Technology* submitted.
- Suomalainen M, Nakano M, Keller S, Boucke K, Stidwill R, Greber U. 1999. Microtubule-dependent plus- and minus end - directed motilities are competing processes for nuclear targeting of adenovirus. *J Cell Biol* 144(4):657-672.
- Swift DL, Montassier N, Hopke PK, *et al.* 1992. Inspiratory deposition of ultrafine particles in human nasal replicate cast. *23:65-72.*
- Tabata Y, Ikada Y. 1988. Effect of the size and surface charge of polymer microspheres on their phagocytosis by macrophage. *Biomaterials* 9:356-362.
- Tjälve H, Mejare C, Borg-Neczak K. 1995. Uptake and transport of manganese in primary and secondary olfactory neurones in pike. *Pharmacol Toxicol* 77(1):23-31.
- Tjälve H, Henriksson J. 1999. Uptake of metals in the brain via olfactory pathways. *NeuroToxicology* 20((2-3)):181-196.
- Tuch T, Brand P, Wichmann HE, Heyder J. 1997. Variation of particle number and mass concentration in various size ranges of ambient aerosols in Eastern Germany. *Atmospheric Environment* 31(No. 24):4193-4197.
- Turetsky BI, Moberg PJ, Arnold SE, Doty RL, Gur RE. 2003. Low olfactory bulb volume in first-degree relatives of patients with Schizophrenia. *Am J Psychiatry* 160(4):703-708.
- Valberg PA, Blanchard JD. 1991. Chapter 36, Pulmonary macrophage physiology: Origin, motility, endocytosis. In: *Treatise on Pulmonary Toxicology --. In: Treatise on Pulmonary Toxicology--Comparative Biology of the Normal Lung.*
- Wojciak-Stothard B, Curtis A, Monaghan W, MacDonald K, Wilkinson C. 1996. Guidance and activation of murine macrophages by nanometric scale topography. *Exp Cell Res* 223:426-435.
- Zheng M, Jagota A, Strano M, *et al.* 2003. Structure-based carbon nanotube sorting by sequence-dependent DNA assembly. *Science* 302:1545-1548.
- Zhu Y, Hinds WC, Kim S, Shen SK, Sioutas C. 2002. Study of ultrafine particles near a major highway with heavy-duty diesel traffic. *Atmospheric Environment* 36:4323-4335.
- Zimmer AT, Baron PA, Biswas P. 2002. The influence of operating parameters on number-weighted aerosol size distribution generated from a gas metal arc welding process. *J Aerosol Science* 33:519-531.



## 8. *Figure Legends*

Figure S-1: Correlation between daily mortality rate and urban particle concentrations during the London smog episodes in the winters of 1958-1972 (*data from Schwartz and Marcus 1990*). Also shown are the regression lines for the steep slope and the shallow slope and the mathematically determined inflection point at  $\sim 125 \mu\text{g}/\text{m}^3$ . This could be explained by the presence of singlet ultrafine particles at lower mass concentrations in the air and aggregated particles at higher mass concentrations (*from Oberdörster 2001*).

Figure S-2: Lung lavage neutrophils 24 hrs. after intratracheal dosing with ultrafine (20 nm) and fine (250 nm)  $\text{TiO}_2$  in rats and mice. Normalization for different particle surface areas and lung weights shows that acute pulmonary cell response is essentially the same in both species (*based on data from Oberdörster et al., 2000*).

Figure S-3: Chemically different NSP can have different effects: Whereas 20 nm particles of both  $\text{TiO}_2$  and  $\text{Al}_2\text{O}_3$  show the significantly greater inflammatory response in the lung when compared to the same mass dose of larger particles, nano-sized  $\text{Al}_2\text{O}_3$  induces a more persistent effect which has not returned to control levels by day 59 post-exposure.

Figure S-4: Inflammatory lung lavage parameters (neutrophils [PMN], protein) in rats within 4 hours after a 15-min. inhalation exposure to ultrafine PTFE fumes. The “adapted” rats had been exposed for 5 minutes on each of 3 days prior to the 15-min. exposure, whereas the “non-adapted” group was sham-exposed to filtered air for 3 days prior to exposure and the “sham” group was exposed to filtered air throughout. The deposited alveolar dose of ultrafine PTFE was estimated to be just  $\sim 65 \text{ ng}$  (*Johnston et al. 1997*).

Figure S-5: Deposition of inhaled singlet 20 nm particles in different generations of the lower human respiratory tract, based on predictions by the MPPD model (Asgharian et al. 1999). Generation 1 (trachea) to generation 16 (terminal bronchioles) represent the tracheobronchial region, generations 16 to 26 are the alveolar region. Deposited mass is expressed as relative units per airway generation (a) or per  $\text{m}^2$  of each generation (b). Although 20 nm particles

have the highest deposition efficiency in the alveolar region (see also Figure 8), the tracheobronchial region receives the highest dose per unit surface area.

Figure S-6: Deposited doses of polydisperse particles with CMD of 20 nm and 250 nm (GSD = 1.7) during a 6-hr. inhalation at  $100 \mu\text{g}/\text{m}^3$  (predicted by MPPD model) in naso-pharyngeal, tracheo-bronchial, and alveolar region of the human respiratory tract during nasal breathing. Although the alveolar region receives the highest dose and the nasal region the lowest, this is reversed when the dose is expressed per unit surface area: the nose, – in this case, has the highest and the alveolar region the lowest dose. Note the consistently higher deposited dose for the polydisperse 20 nm aerosol in all regions.

Figure S-7: Pulmonary inflammation and interstitial particle translocation 24 hrs. after instillation of 12 - 250 nm  $\text{TiO}_2$  particles in rats; carbon black (20 nm) used as comparison. (a) Particle size and dose-dependent inflammatory cells in lung lavage: note the lower response of the two larger doses of 12 and 20 nm-sized  $\text{TiO}_2$ , in contrast to 20 nm carbon black particles; (b) particle size and dose-dependent protein in lung lavage: note the linear increase of this inflammatory parameter with increasing doses for all particle types; (c) size and dose-dependent interstitial translocation; note the lower translocation of carbon black particles; (d) particle size dependent translocation of  $\text{TiO}_2$  particles (Oberdörster et al., 1992).

Figure S-8: Potential target sites and effects of inhaled NSP based on experimental results with ambient UFP inducing oxidative stress. Translocation and effects are highly dependent on particle surface properties, biopersistence and bioavailability of particle constituents, and are further modified by host factors such as age, disease state, and co-pollutants.

## 9. Tables

Table S-1: Airborne Ultrafine/Nanoparticles: Workplace and Environment.

Table S-2: Up- and down-regulated genes from initial largemouth bass suppressive subtractive hybridization studies, after fish were exposed to 0.5 ppm  $\text{nC}_{60}$  for 48 hours.

**Table S-1**

***Airborne Ultrafine/Nano Particles: Workplace and Environment***

<b>Sources</b> →	<b>Exposure</b> →	<b>Dose</b> →	<b>Response</b>
<u>What are they?</u>	<u>What levels?</u>	<u>How much is retained?</u>	<u>Physiological or adverse?</u>
<b><u>Indoors</u></b> <i>heated surfaces frying broiling grilling electric motors</i>	<b><u>Exposure Routes</u></b> <i>inhalation ingestion dermal</i>	<b><u>Dosemetric</u></b> <i>mass number surface</i>	<b><u>Epidemiologic Studies</u></b> <i>ambient UFP susceptibles only? mortality/morbidity (respiratory, cardiovascular)</i>
<b><u>Outdoors</u></b> <i>urban air internal combustion power plants incinerators gas-to-particle convers. forest fires airplane jets recreation (ski waxing)</i>	<b><u>Concentration</u></b> <i>ng/m<sup>3</sup> - mg/m<sup>3</sup> 10<sup>2</sup> - &gt;10<sup>6</sup> part./cm<sup>3</sup></i>	<b><u>Deposition</u></b> <i>respiratory tract: ventilatory and anatomic parameters</i>	<b><u>Clinical Studies</u></b> <i>lab. generated UFP ambient UFP healthy/susceptibles (respiratory, cardiovascular)</i>
<b><u>Workplace</u></b> <i>metallurgy (fumes) welding polymer fumes nanotechnology (biomed. electronics) nanotubes</i>	<b><u>Duration</u></b> <i>minutes hours days continuous/peak</i>	<b><u>Disposition</u></b> <i>within respiratory tract extrapulmonary organs disease state</i>	<b><u>Animal Studies</u></b> <i>lab. generated UFP Ambient and occupational UFP compromised animal models (respiratory, cardiovascular, CNS) mechanisms</i>
	<b><u>Location</u></b> <i>distance from source wind direction</i>	<b><u>Physico-chemical Properties</u></b> <i>organics, inorganics metals crystalline, amorphous surface area solubility (water, lipid)</i>	<b><u>In vitro Studies</u></b> <i>mechanisms oxidative stress cellular/molecular</i>

Table S-2

# TOXICOLOGY OF ENGINEERED NANOPARTICLES (NP)

<b>Exposure</b>	<i>Mechanisms of</i>  <i>Intake, Uptake</i> <i>Determining Dose</i>	<b>Dose</b>	<i>Biokinetics</i> <i>Mechanisms of</i>  <i>Cellular, Molecular</i> <i>Events</i>	<b>Response</b>
<b>Which medium?</b> <i>air</i> <i>water</i> <i>food</i>		<b>How much?</b>  <b>Which dosemetric?</b> <i>mass</i> <i>number</i> <i>surface</i> <i>(size, chemistry,</i> <i>charge, shape)</i>		<b>Portal of entry effects</b> <i>vs.</i> <b>Remote organ effects?</b>  <b>Neutral?</b>  <b>Desirable?</b> <i>therapeutic</i> <i>diagnostic</i>
<b>What concentration?</b>		<b>Where retained?</b> <i>(Disposition)</i> <i>organ</i> <i>cell</i>		<b>Toxic?</b> <b>oxidative stress</b> <b>disrupting function:</b> <i>organ</i> <i>cell</i> <i>molecular pathway</i> <b>immune function</b>
<b>Which route?</b> <i>inhalation</i> <i>ingestion</i> <i>dermal</i> <i>injection</i>		<b>How persistent?</b>		

***Modifying Factors: Age, Disease (Susceptibility)***

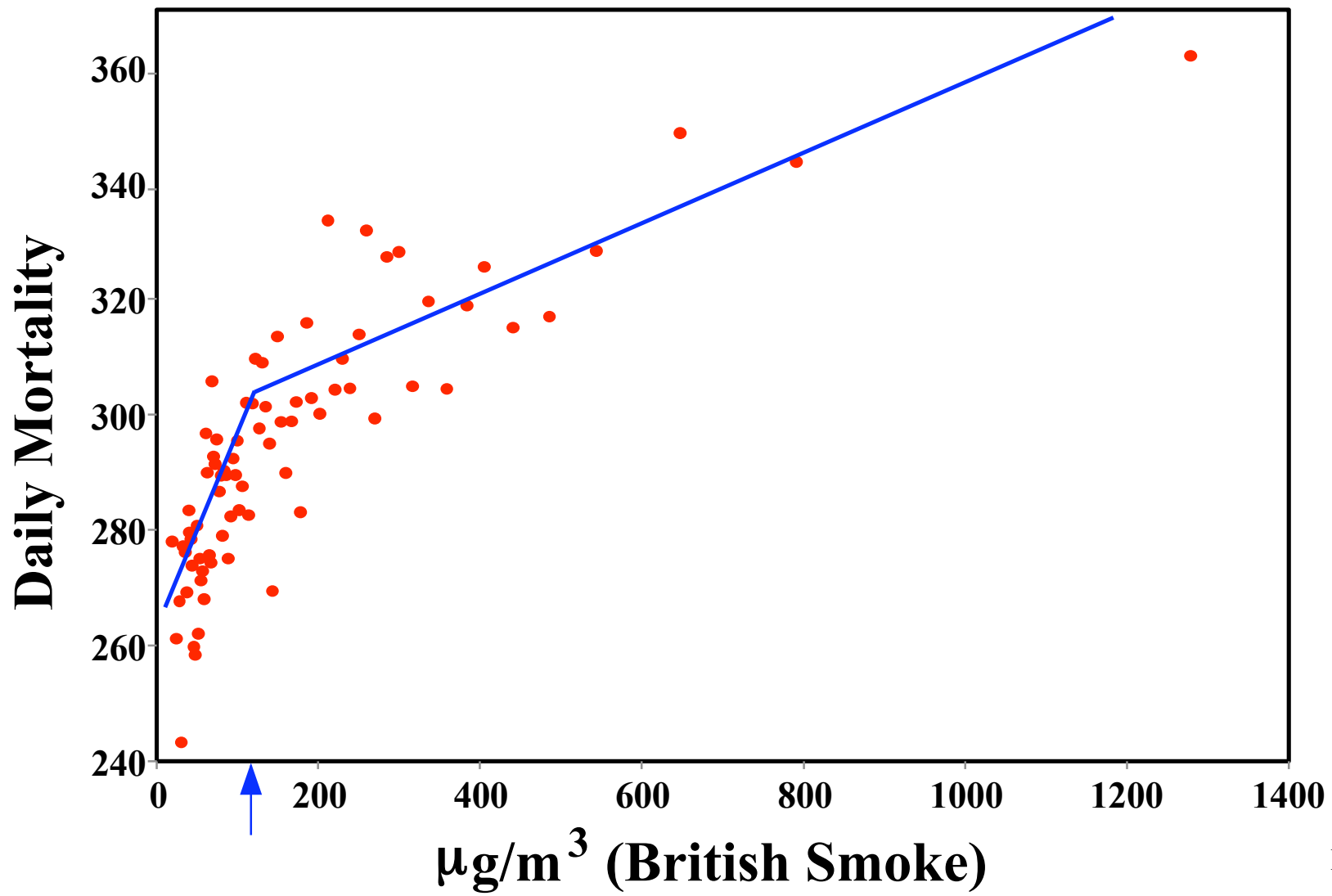
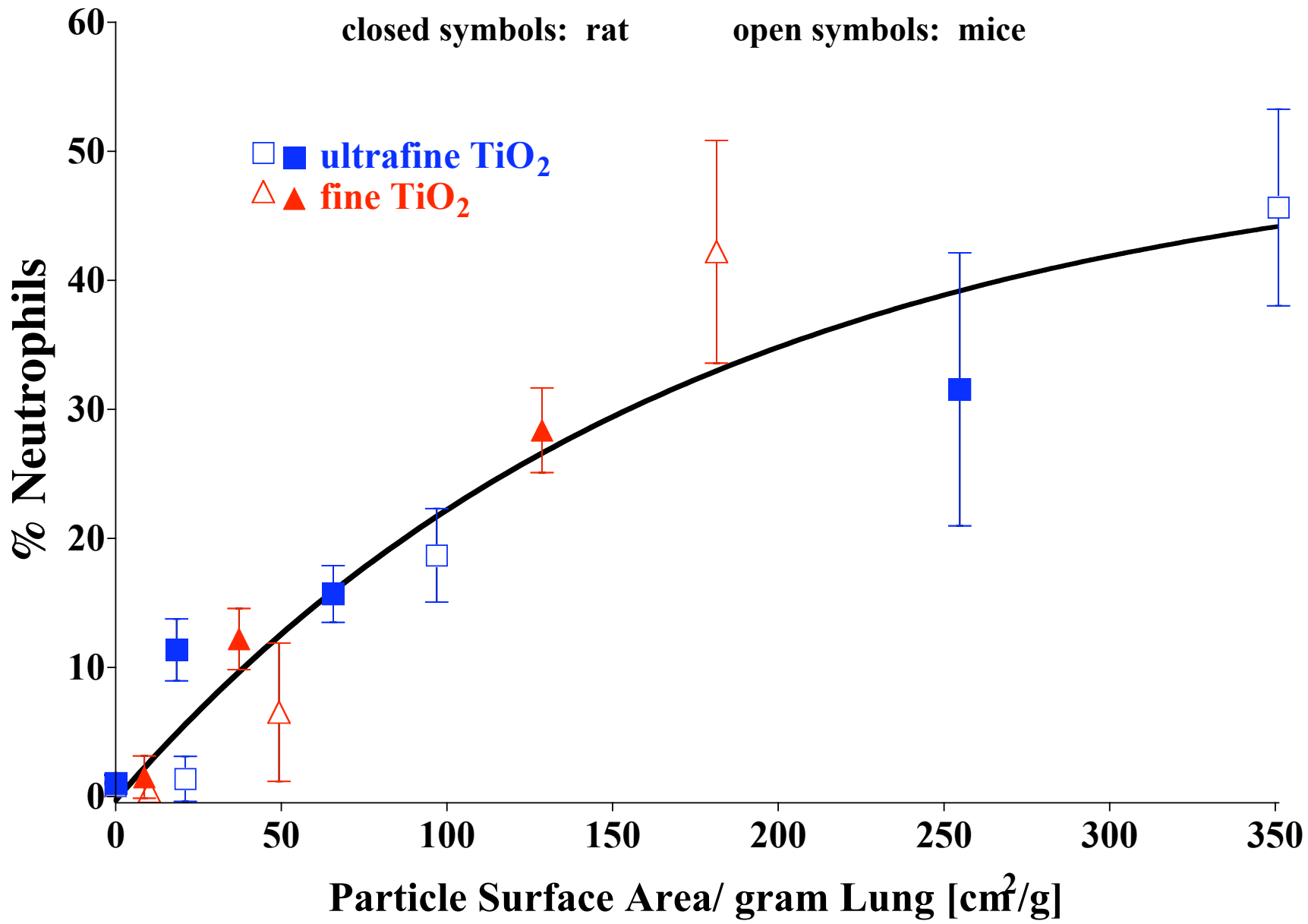


Figure S-1

# Percent of Neutrophils in BAL 24 hrs after Instillation



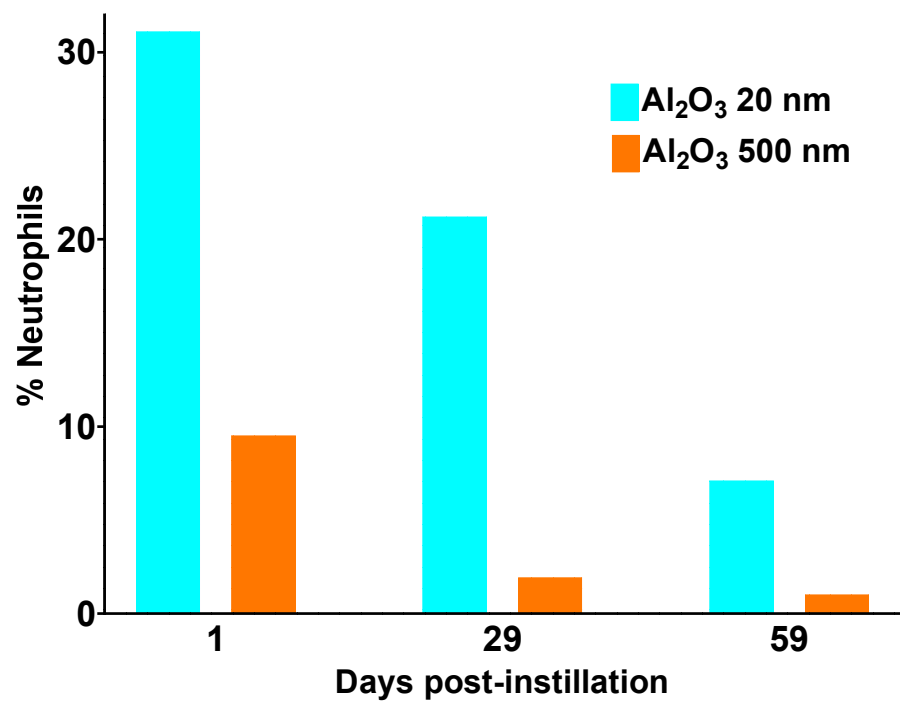
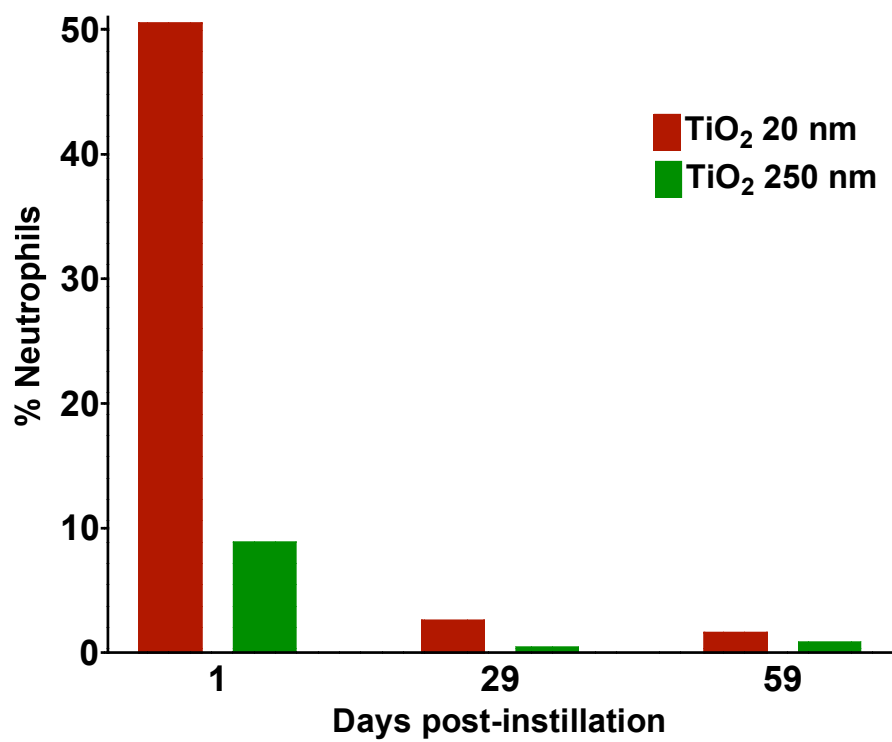


Figure S-3

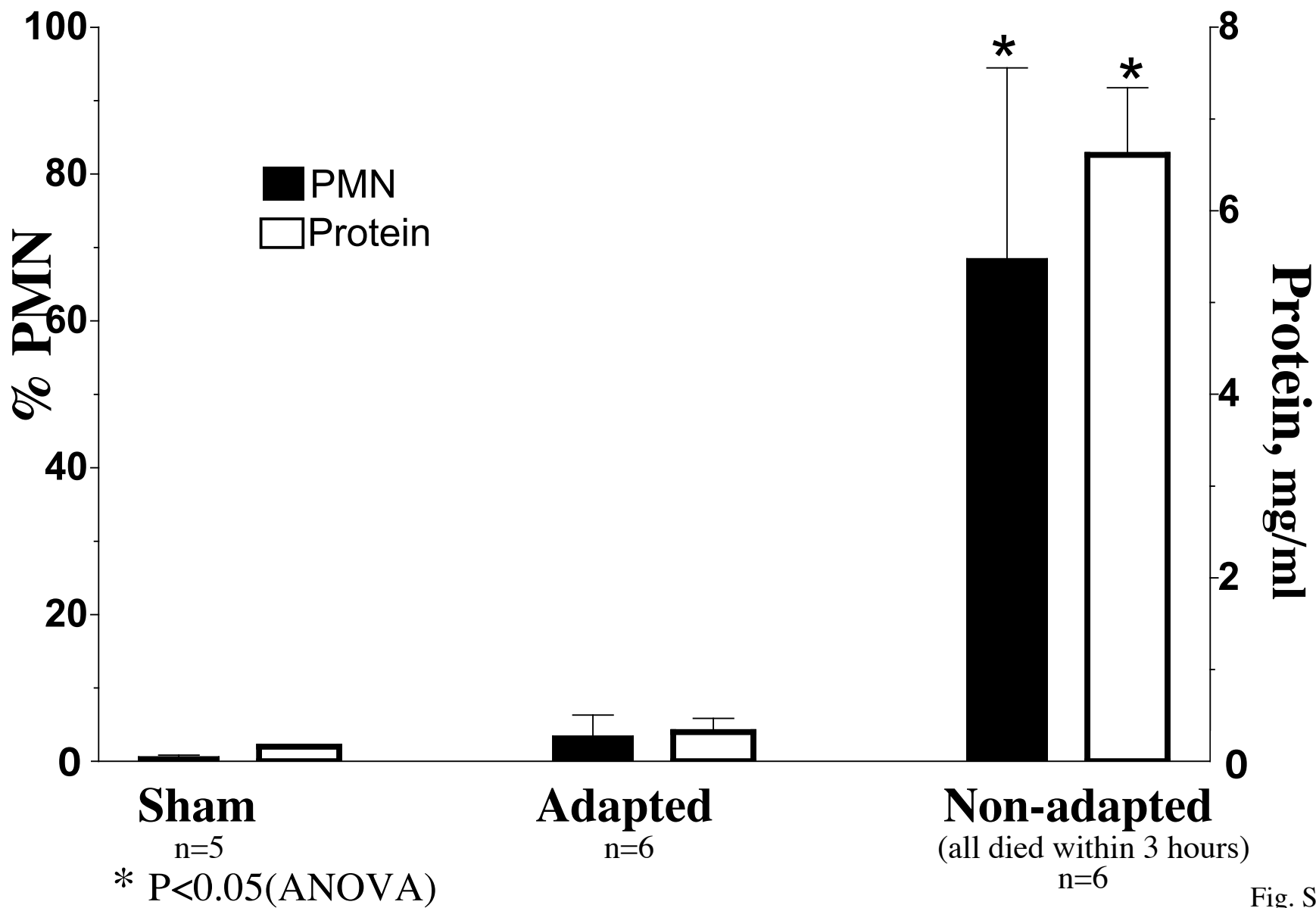
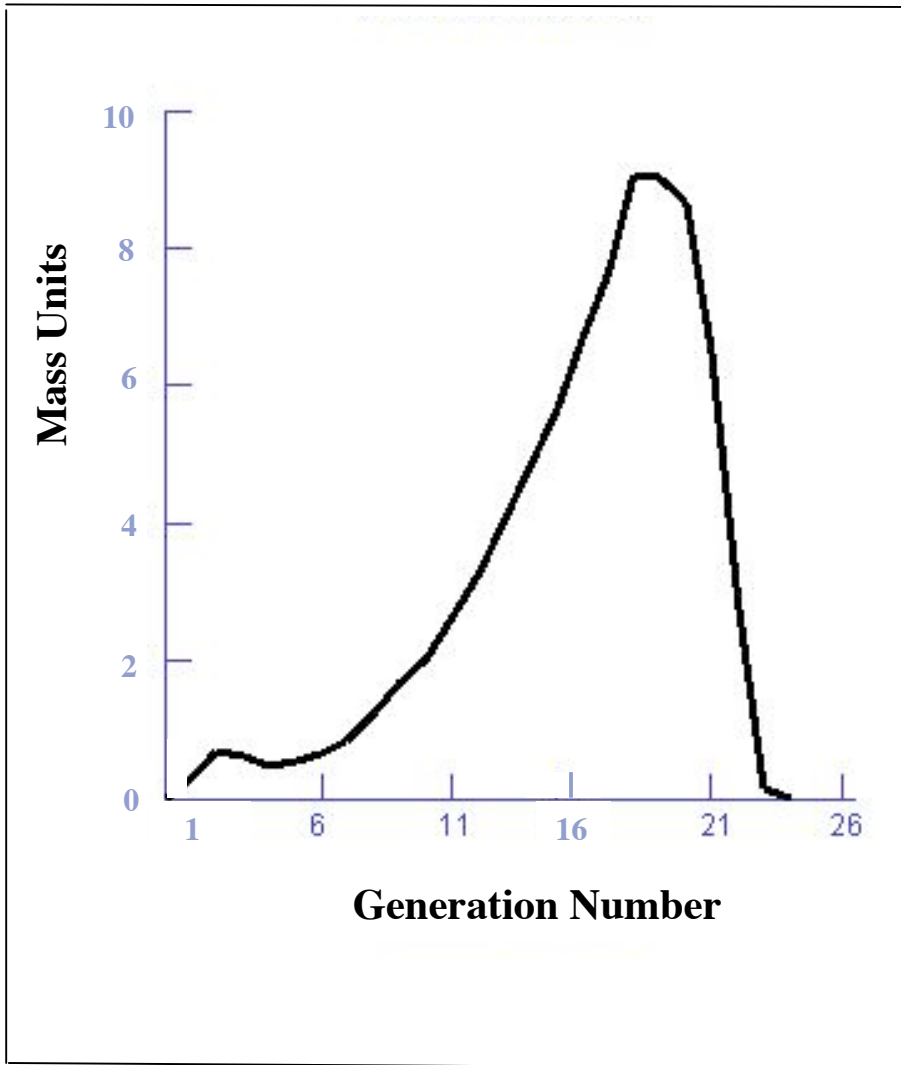
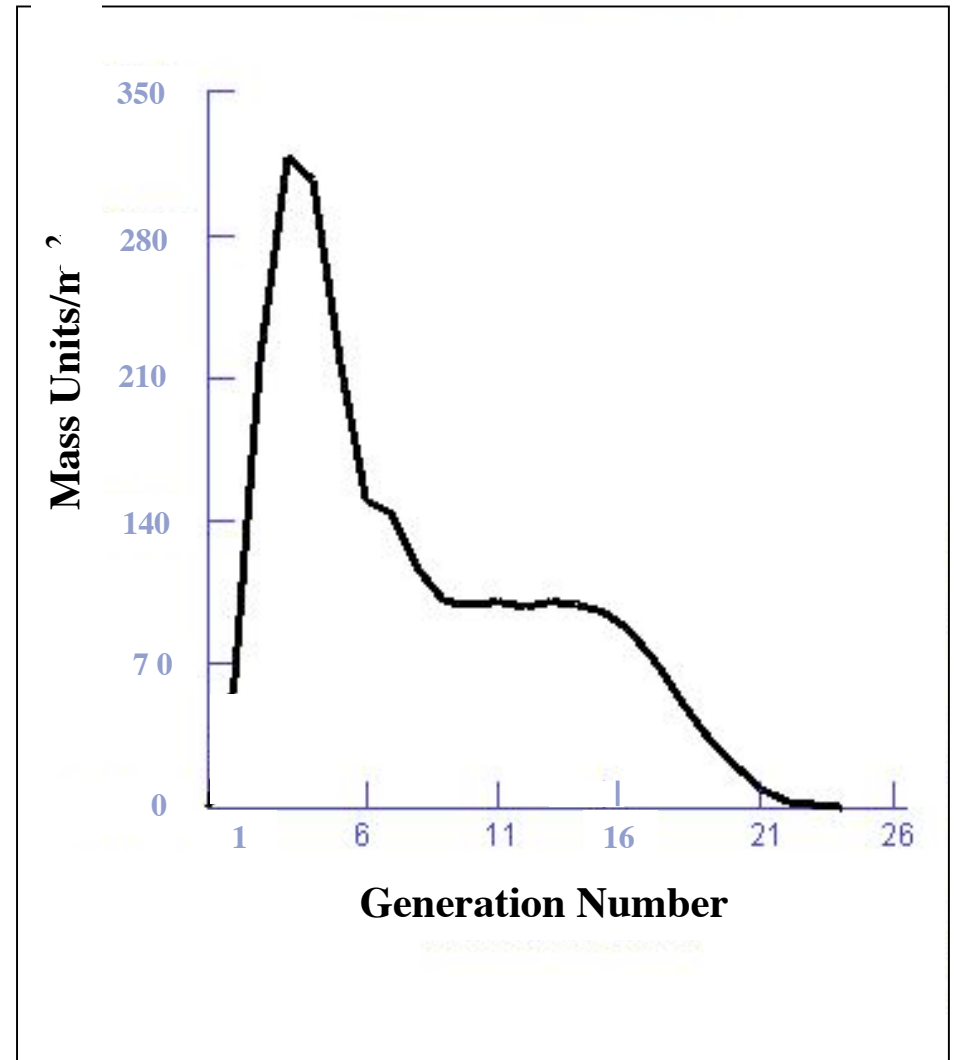


Fig. S-4



**Particle Mass per Generation**



**Particle Mass per Unit Surface Area**

Figure S-5

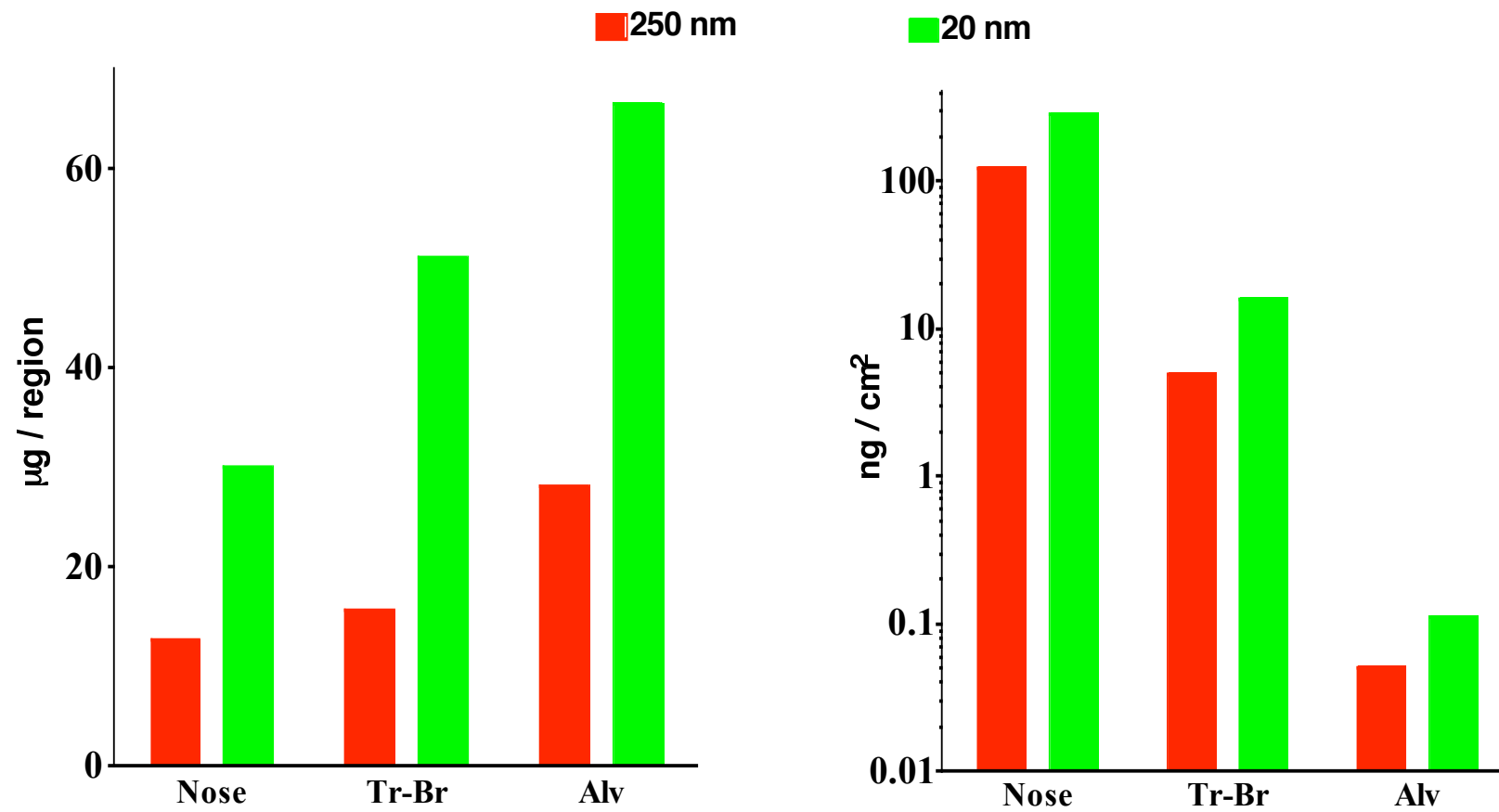


Figure S-6

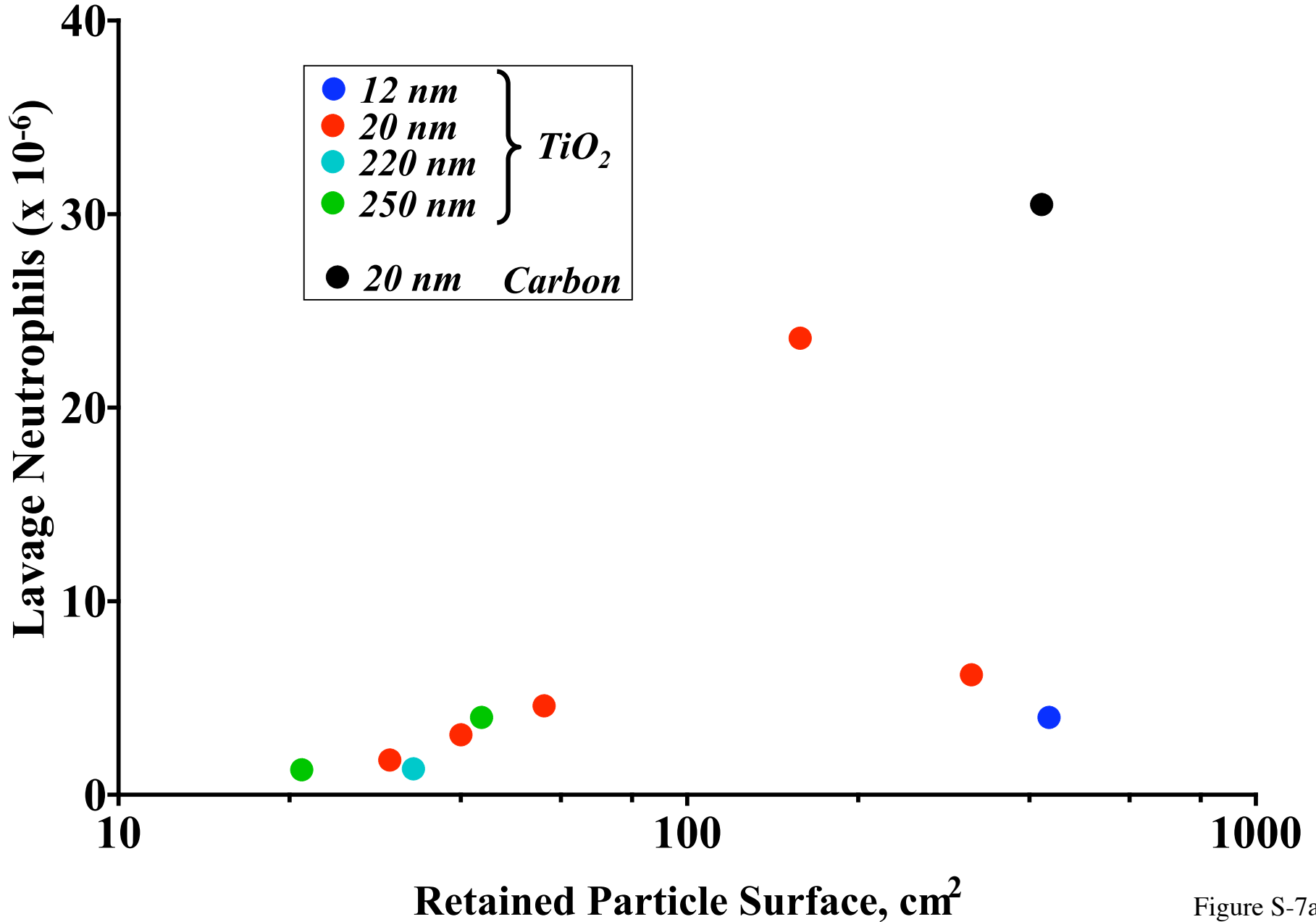


Figure S-7a

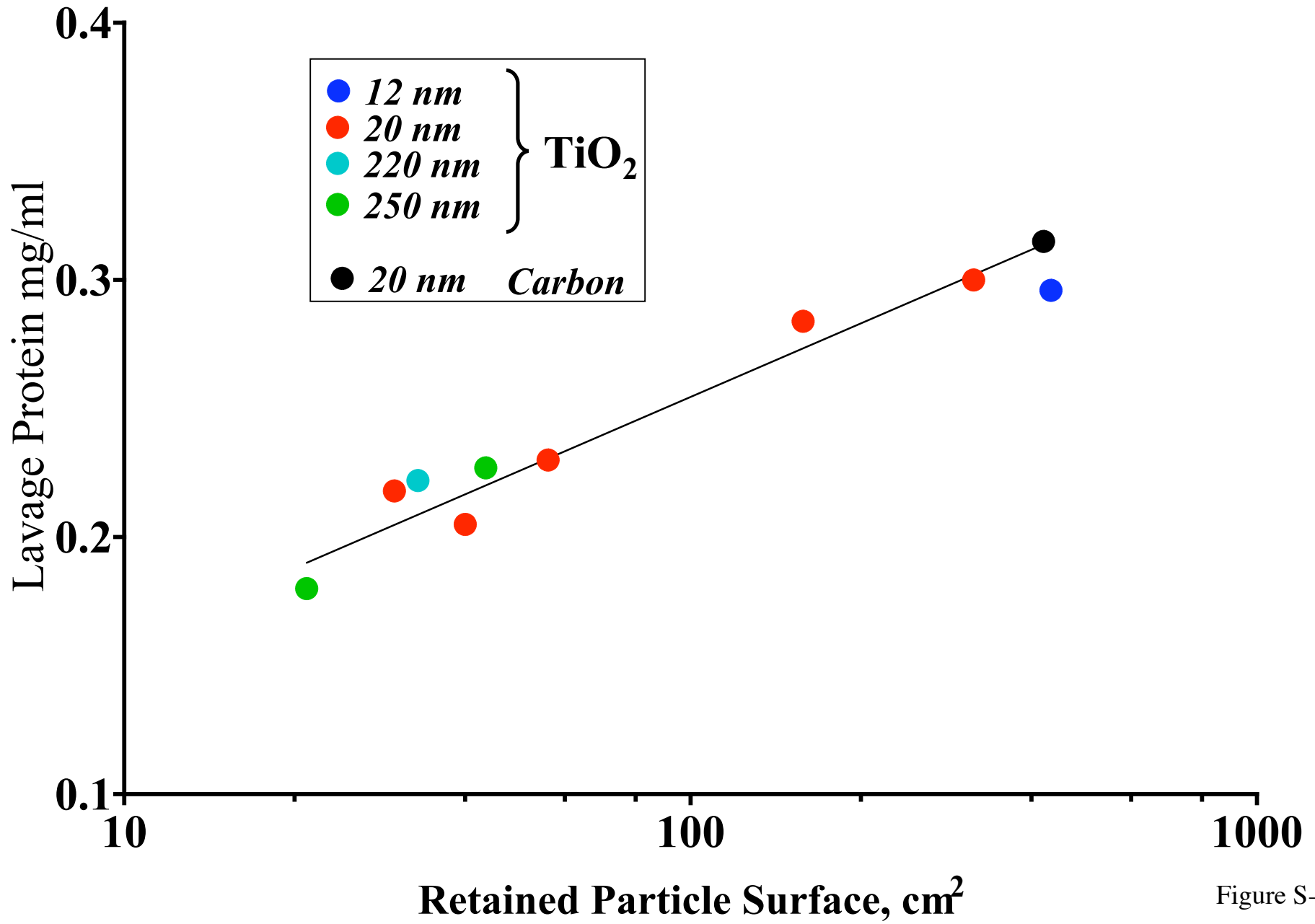


Figure S-7b

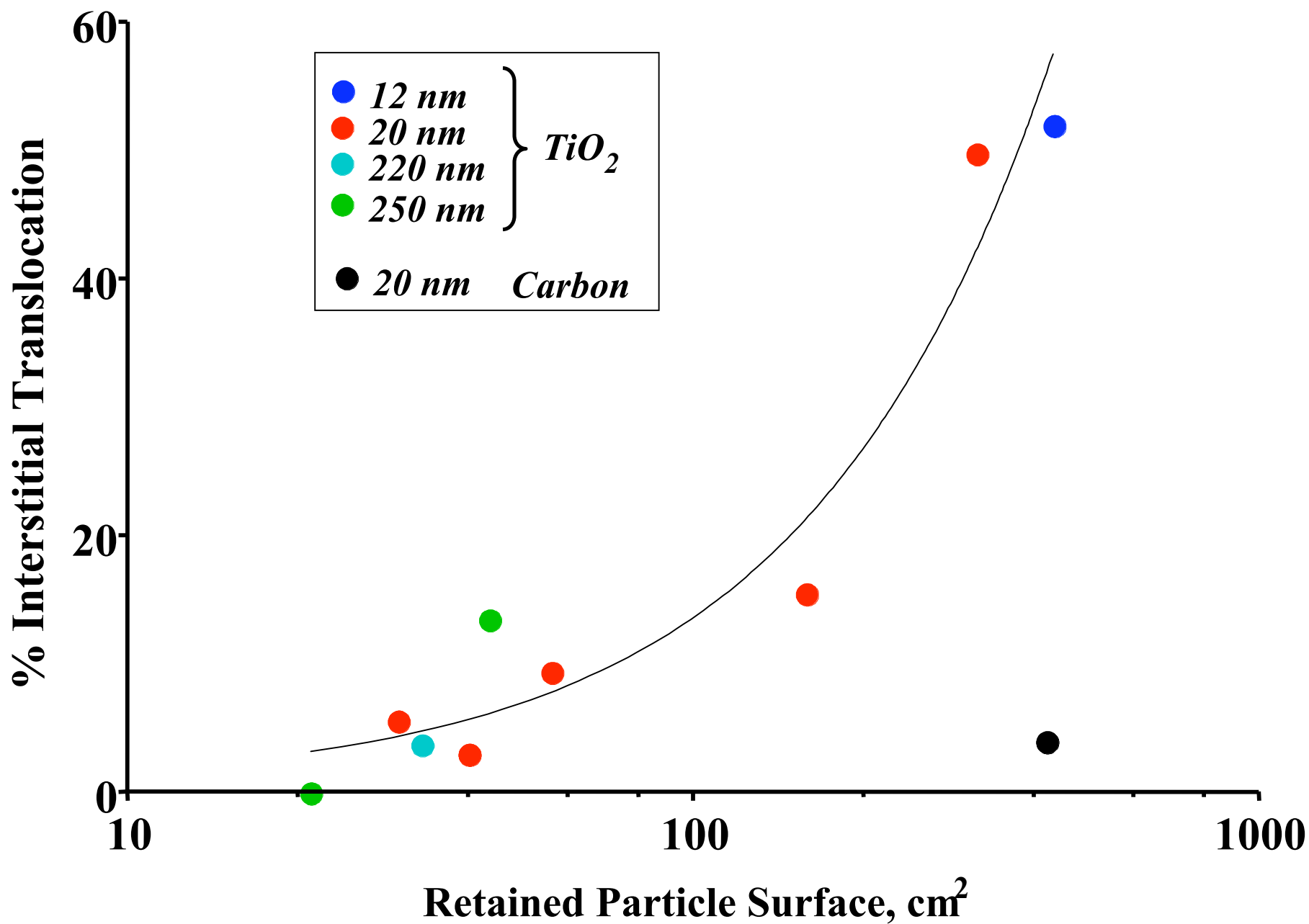
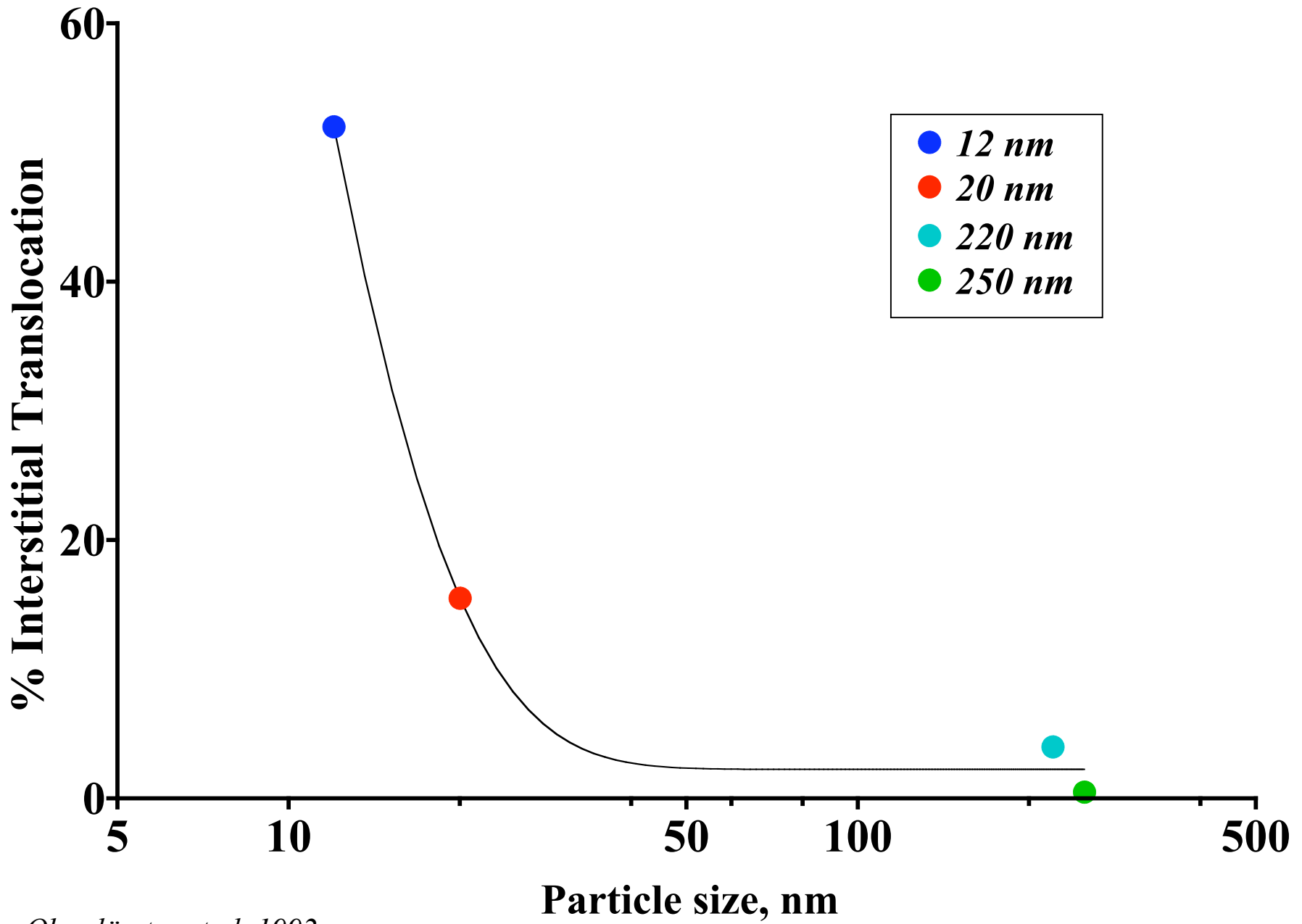


Figure S-7c



*Oberdörster et al, 1992*

Figure S-7d

# Ultrafine Particles

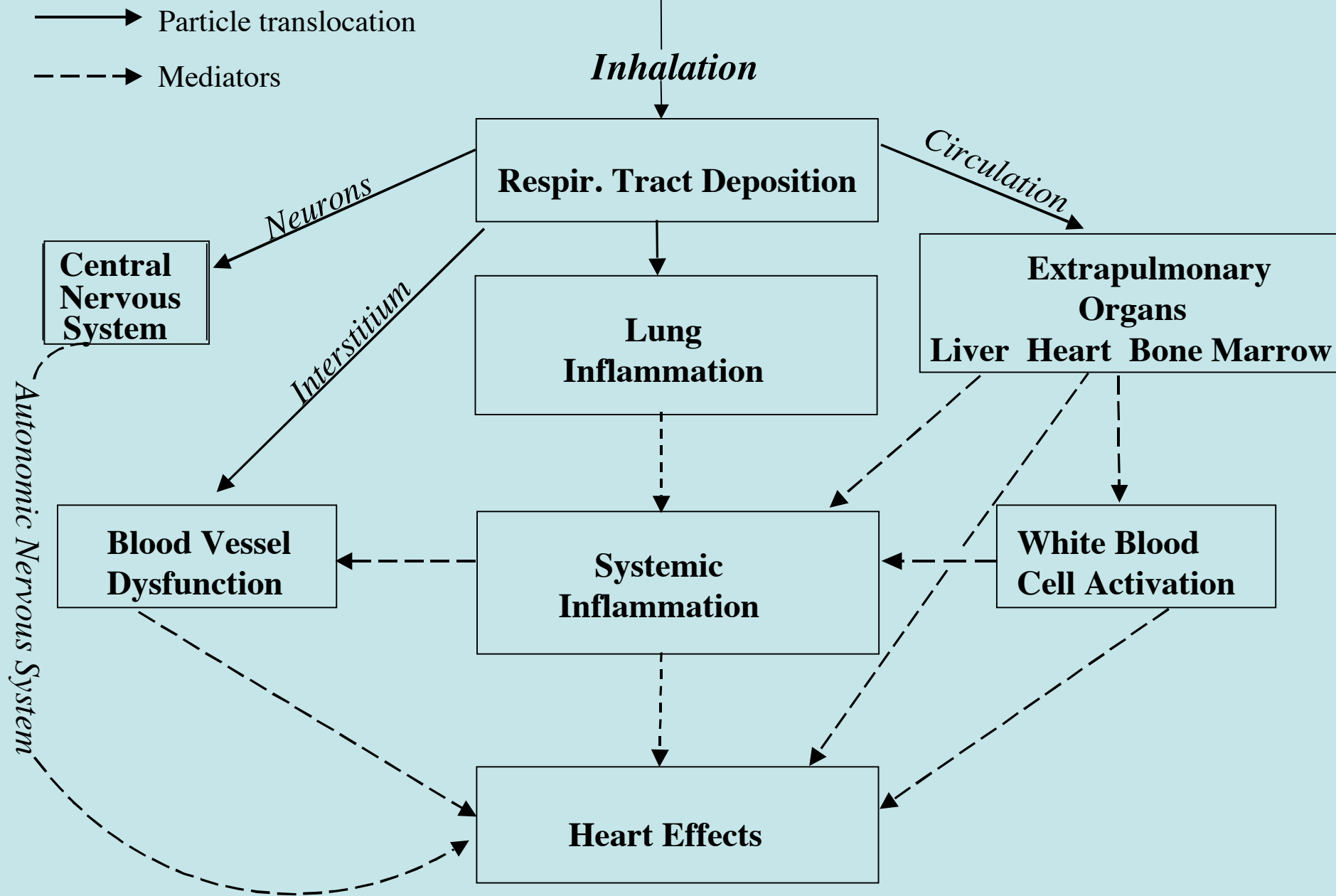


Figure S-8

**Modifying factors: Gender, underlying disease, co-pollutants**